TR-10
1967

On the Feasibility of Precisely Measuring the Properties of a Precipitating Cloud with a Weather Radar

R.C. Runnels

Texas Water Resources Institute

Texas A&M University

ON THE FEASIBILITY OF PRECISELY MEASURING THE PROPERTIES OF A PRECIPITATING CLOUD WITH A WEATHER RADAR

By

Robert Clayton Runnels

TECHNICAL REPORT NO. 10

DECEMBER, 1967

This study was partially supported by the Office of Water Resources Research, The Department of the Interior under P.L. 88-379, Project A-002-TEX.

FOREWORD

The ultimate goal of our investigations is to gain a better understanding of the rainfall process in the State of Texas. Particular emphasis has been placed on the use of weather radar in these investigations.

This study is the result of an effort to gain an understanding of the instrumental accuracy of a weather radar when such a radar is used to measure the water concentration in clouds. From the areal and temporal variations in water concentration it is possible to infer the intensity of rainfall at the surface of the earth in addition to a better understanding of the mechanism of rainfall formation.

ACKNOWLEDGMENTS

This study was supported in part by Project A-002-TEX of the Office of Water Resources Research, The Department of the Interior, through the Water Resources Institute of Texas A&M University.

The author wishes to express appreciation to the following faculty member of Texas A&M University for their assistance: Drs. V. E. Moyer, K. C. Brundidge, and R. A. Clark of the Department of Meteorology, Prof. R. O. Reid of the Department of Oceanography, and Dr. R. E. Basye of the Department of Mathematics. A special indebtedness is owed to Mr. Fred A. Schmer of the Water Resources Institute for his valuable assistance.

ABSTRACT

In this paper the results of an investigation are presented that are concerned with the feasibility of employing a weather radar to make precise measurements of the properties of a precipitating cloud. A schematic cloud is proposed as a model for interpreting the interaction of the radar energy with the cloud. Point values of the liquid-water concentration are estimated from measurements of the received power. The measurements were made under conditions which minimized errors arising from attenuation of the radar signal and a radar beam which is not completely filled with raindrops.

A continuity equation for liquid-water concentration is developed. The vertical speeds at the core of convective clouds are related to the spatial and temporal variations of the liquid-water content by means of this equation. The version of the continuity equation developed in this study represents an improvement over forms used previously. The new version accounts for the downward development of a radar echo at speeds faster than the fall speed of raindrops. This echo development is caused by the coalescence mechanism.

An error analysis is performed and it indicates that the percentage error of the measurements of the liquid-water concentration may be as much as 102.4%. The fractional error of the vertical speeds is ± 1391.4% which results from the compounding

of the experimental errors of the terms in the continuity equations.

To check the estimated magnitudes of the experimental errors a case study was performed. The echoes of 23 convective clouds were studied and 695 observations of liquid-water concentration were obtained. The observed magnitudes indicate that these estimates are of the correct order. The values of vertical speeds also indicate that the estimated error of this quantity is indeed large.

Possible methods for reducing the experimental errors are considered. This examination indicates that reasonably accurate measurements of liquid-water concentration can be made if high experimental standards are maintained. The use of calibrating instruments which are very accurate together with good experimental control may permit a reduction of the percentage error to less than 20%. However, this study indicates that attempts to measure vertical speeds accurately by use of the continuity equation may not be too successful.

TABLE OF CONTENTS

LIST OF FIGURES

LIST OF TABLES

LIST OF SYMBOLS

a	drop diameter
a_M	diameter of the smallest drop that can be detected by radar
a_0	median-volume diameter
a_{50}	median-reflectivity diameter
A	term appearing in Equation (24)
b	parameter in the Marshall-Palmer distribution
B	term appearing in Equation (24)
C, C_1, C_2	radar constants
$\hat{C}$	three-dimensional wind vector
C_D	drag coefficient
D	diffusivity of water vapor in air
e_s	saturation vapor pressure
E	collection efficiency; squares of the contribution to the fractional error of M
f	ventilation factor; functional notation used in Equation (44)
F	functional notation used in Equation (38)
g	acceleration due to gravity
G	antenna gain
G_f	generating function
h	pulse length
H	height above mean sea level
$\hat{k}$	unit vector positive toward the zenith

K	coefficient of thermal conductivity
K^2	dielectric factor used in Rayleigh scattering theory
L	latent heat of evaporation
m	mass concentration of drops whose diameters are less than 100μ
M	mass concentration of drops whose diameters are greater than 100μ
M'	total concentration of the mass of liquid water
n	number of drops per unit volume per class interval
N	total number of drops per unit volume
N_o	parameter in the Marshall-Palmer distribution
P_d	average received power in decibels
P.E.	probable error
P_{min}	minimum detectable power
$\bar{P}_r$	average received power
P_t	transmitted power
Q	source function
r	range
R	rainfall rate
R_d	specific gas constant of dry air
R_w	specific gas constant of water vapor
s	absolute error
S	saturation ratio; fractional error
S.D.	standard deviation

t	time
T	temperature
u, v, w	wind speeds in the positive x-, y-, and z- directions, respectively
V	terminal fall speed
$\bar{V}$	speed of the drop with the median-volume diameter
$\langle V \rangle$	ensemble volume-mean speed
x	maximum drop diameter
x, y, z	Cartesian space coordinates
Z	radar reflectivity factor
α, β	dummy variables of integration representing drop diameters
γ	critical diameter of drop
Δ	difference operator
ϵ	complex index of refraction
η	total back-scattering cross section per unit volume
θ	horizontal beam width
θ_w	wet-bulb potential temperature
λ	wave length
ρ	air density
ρ_L	density of liquid
ρ_s	saturation vapor density
σ	back-scattering cross section
τ	coalescence-transfer term

φ	vertical beam width
χ	liquid-water content of small drops
ω	elevation angle of radar beam
∇	del operator

CHAPTER I

INTRODUCTION

Nature of the Problem

Before the meteorologist can attempt sagaciously to modify rainfall from clouds or before he can predict with any degree of certainty the distribution of unmodified rain over a geographical area, he must gain an understanding of the thermodynamic and kinematic principles that describe the formation and subsequent evolution of this rain. In the study of the physical processes of precipitation, an important consideration is the delineation of the spatial distribution of water in the cloud and the variations of this distribution with time.

The primary purpose of this study was to investigate the feasibility of using a weather radar to obtain precise measurements of the formation of rain in cumulus clouds. A secondary objective was the accurate measurement of the vertical velocities in a cloud that are related to the process of rain formation. Convective clouds form as the result of the expansion and consequent cooling of ascending air. Cloud droplets will form by the condensation or sublimation once a sufficiently high relative humidity is reached. In the case of clouds which extend to heights in the atmosphere where temperatures are much less than 0C, an important mechanism for the formation of rain is one in which drops begin their life as ice crystals and then grow

rapidly at the expense of surrounding water drops. When the ice crystals attain a sufficient size, they fall from the upper regions of the cloud and melt upon falling through the isothermal surface whose temperature is 0C. To account for rain which falls from clouds that do not reach the height of the 0C-isothermal surface, another mechanism appears to be operative. In these so-called "warm" clouds, drops form initially as small droplets by condensation and a small proportion of their number grows further by colliding with the remaining droplets. Growth of the droplets to raindrops will occur if there are adequate collisions and coalescence between the smaller cloud droplets. The probability of a collision is enhanced by vertical velocities that are strong enough to support the droplets and maintain a relatively high concentration in the cloud. Since the time for precipitation to appear at the ground is dependent on the vertical air speeds, the measurement of the rate of ascent was deemed to be important. The technique used to measure the vertical velocities was an extension of the method used by Runnels [1962] and Clark [1964]. The measurements of the water content of a cloud (and the changes of this water content) were made by using a weather radar in the Department of Meteorology of Texas A&M University. The technique used to measure the water content of the cloud was a special case of the general scattering problem in which electromagnetic waves interact with a collection of particles and a portion of the scattered energy is measured.

From the spatial distribution of the scattered energy it is possible to deduce some of the physical properties of the scattering particles. The weather radar irradiates a portion of a cloud and measures the energy scattered in the direction of the radar set. The energy received at the radar site is proportional to the concentration of particles in the irradiated volume. An advantage in using a weather radar to measure the properties of a cloud is that the sampling may be performed without disturbing the sampled volume.

Previous Studies

The first study to employ radar techniques to obtain a broad picture of a precipitating cloud was the Thunderstorm Project carried out in 1946-47 by Byers and Braham [1949]. Data collected during this project were analyzed by Battan [1953]. He concluded that precipitation could be initiated in clouds over the continental United States, in the summer, by a process involving only droplet growth by coalescence. Bowen [1950] drew a similar conclusion from radar studies of cumulus clouds in Australia. Atlas [1954] found that there is a general correlation between rainfall intensity and the parameters which describe the distribution of drops with size. He used measurements from six types of clouds which were observed in New England, and with these data he was able to estimate cloud parameters from radar echo-intensities.

The cumulus clouds that form in the southeastern part of Texas have characteristics that are intermediate between clouds of continental and maritime origin. Studies of maritime clouds over the tropical ocean near Puerto Rico have been made by the Cloud Physics Group of the University of Chicago [Byers and Hall, 1955]. Squires [1956] examined both continental and maritime cumuli in the area of the trade winds. Both of these investigations pointed out that rain will fall more easily from maritime clouds than from continental clouds of the same height. Observations show that the maritime clouds contain drops with larger diameters than the continental clouds. The presence of the larger drops enhances the possibility of shower formation by coalescence.

In recent years the University of Chicago group has made studies by radar of the sequence of events following the first appearance of echoes in continental cumulus clouds that developed over Missouri [Byers, 1965]. Studies of subtropical cumuli have been made by the Radar Meteorology Section of the Department of Meteorology of Texas A&M University since the late 1950's. Prior to the work of Clark [1964], these studies were made with a radar of 3.2-cm wavelength. At this wavelength, attenuation of the radar signal by regions of intense rainfall can vitiate the results. Clark used a 10.3-cm wavelength radar in addition to the 3.2-cm radar mentioned above. Since the 10.3-cm signal experiences negligible attenuation when passing through moderate

to heavy rainfall, Clark attempted to measure the water content of a cloud by comparing the power received at the two wavelengths. He concluded that the values of received power could not be measured with sufficient accuracy to give reliable estimates of the water content of the cloud. Atlas [op.cit.] indicated that it is necessary to measure values of received power with an accuracy of the order of ± 0.5 db in order to obtain reliable estimates.

The paper by Atlas is one of the few in the literature of Radar Meteorology that considers the random error involved in the measurement of the water content of a cloud. Discussions of errors are usually limited to a consideration of the systematic errors inherent in the measuring apparatus and the method used to measure the quantity under consideration. A paper by Probert-Jones [1962] contains a summary of the systematic errors encountered by many of the research groups using radar to obtain quantitative measurements of rain. In general, these errors have caused an underestimate of the amount of water at the point where the measurement is made. The systematic errors that are present when there is attenuation of the radar signal were considered by Atlas and Banks [1951] and Hitschfeld and Bordan [1954]. Since large random errors can affect the results as seriously as systematic errors, it became apparent that an analysis of the random errors which arise during the measuring process must be performed before an estimation of the variability of the measurements can be made.

The 10.3-cm radar used by Clark was modified during 1964-65 to improve its capabilities to measure the properties of precipitating volumes of cloud. The data used in this study were the first collected with the modified radar that employed the reflectivity-height-run technique. This technique is described in Chapter V.

Schematic Cloud

Each cloud has a distinctive appearance and particular characteristics. The clouds, however, can be grouped according to certain general types which resemble one another in their essential traits. It is possible to depict the growth and general characteristics of a class of clouds. Such a depiction, of necessity, will be schematic; it will not fit exactly any one particular case but will be a description of what is common to a whole class. The "schematic" cloud is, therefore, an abstract of individual characteristics.

To be useful, any mathematical model of a physical phenomenon, such as the schematic cloud, should be accurate enough for the purposes of the investigation but simple enough to be manipulated without too much difficulty. The mathematical description of the schematic cloud used in this study consists of features which are applicable to clouds in general and some particular features that apply to subtropical cumuli.

Some general characteristics. The clouds examined during

the course of this study were cumulus clouds of such size that the raindrops could be detected by a 10.3-cm radar signal. At this wavelength the process of droplet growth must proceed almost to the point of rainfall before a radar echo will be seen [Braham, 1952]. All of the clouds which were studied were within a range of 50 mi of College Station, Texas. The most extensive study of the characteristics of echo-producing clouds in this area was performed by Clark [1960]. The clouds examined by Clark were of the same type as the ones studied in the present investigation. His study indicated the following features: the area of the initial formation of rain was either astride the level in the cloud where the temperature is 0C or beneath this level by depths ranging down to 4000 ft, the average altitude reached by the tops of the growing echoes was 16,000 ft, and the temperature at the top of 88 per cent of the echoes was warmer than -10C. The results of this study indicate that the phase of precipitation of the schematic cloud should be the liquid one, since it is generally known that raindrops may remain in the liquid phase at temperatures as low as -15C [Ludlam, 1951].

Description of the schematic cloud. The properties of the schematic cloud will be stipulated on the basis of a unit volume. Perhaps the most important feature of a volume of cloud is the distribution with size of the drops which comprise the cloud. If the drop-size distribution is known, the total water content and the radar characteristics of the volume may be determined

readily. Measurements of drop-size distributions have been made in clouds by aircraft and at the ground by collecting either the drops in a shower or replicas of these drops. Reviews of these measurements are found in the monographs of Fletcher [1962] and Byers [1965]. Drop-size distributions which are representative of rain showers at a subtropical location (Miami, Florida) have been reported by Mueller [1962]. When the spatial and temporal fluctuations in the drop-size distributions are eliminated by averaging, a persistent feature of these distributions is the exponential decrease of the concentration of drops as the diameter increases. Several investigators have attempted to fit empirical relations to the observed distributions. Fletcher [op.cit.] has made a review of these drop-size distributions. An investigation of these relations and their applicability to radar observations of subtropical precipitation was made by Fanning [1965]. He concluded that a distribution of the form

$$n(a) = N_0 \exp(-ba) \qquad (1)$$

represented the drop-size spectrum in subtropical clouds as well as any of the other empirical relations. In Equation (1) $n(a)da$ is the number of drops per unit volume with diameters between a and $a + da$, N_0 is a constant, and b is an empirical factor which is proportional to the analytical slope of the distribution. The drop-size distribution expressed by Equation (1) was proposed by Marshall and Palmer [1948] (hereafter referred to as the M-P distribution) to fit data collected at the ground. They

found that b is related to the rainfall rate, R, by

$$b = 41R^{-0.21}, \tag{2}$$

where b is in units of cm^{-1} and R is in units of mm hr^{-1}. The constant N_0 was assigned the value 0.08 cm^{-4}, which is typical of most rates of rainfall. Fanning's work [op.cit.] indicated that N_0 may vary with the rainfall rate, but Kessler [1963] has shown that the fluctuations in the value of N_0 must be several orders of magnitude before significant changes are produced in rainfall rates and water content. Since this study was concerned with quantities that can be expressed as higher moments of Equation (1), the choice of N_0 is not too critical. The M-P distribution overestimates the number of drops with small diameters, but this is not serious for our purposes since the contribution of these smaller drops to the total water content is very small.

We stated previously that the data which led to the M-P distribution were obtained at the ground. A question arises concerning the applicability of such a ground-based distribution to conditions in a cloud. Two main factors influence the raindrops in their fall to the ground. Below the base of the cloud, there is a tendency for the drops to evaporate in the unsaturated air. This effect will tend to decrease the number of small drops in the distribution. The other factor affecting the distribution is the coalescence of drops with each other. This will tend to increase the number of large drops. The problem

of applying ground-based observations to conditions in a cloud has been reviewed by Fletcher [op.cit.]. The majority of the investigators of this problem have concluded that changes in the drop-size distribution are not very great as the drops fall from the base of the cloud. Rigby et al. [1954] found the distribution observed at the ground to be the same as the distribution found aloft in a precipitating cloud. Accordingly, it seemed reasonable to assume that the M-P distribution represents the average conditions in our schematic model of a subtropical cloud.

The M-P distribution is limited by a largest diameter, x. Stephens [1962] showed that the largest diameter in the M-P distribution, where $N_0 = 0.08$ cm^{-4}, was related to the rainfall rate by

$$x = 23R^{0.213}, \tag{3}$$

where x is in units of cm and R is in units of mm hr^{-1}. Elimination of R between Equation (2) and (3) gives

$$x = 9.95b^{-1.014}. \tag{4}$$

In Equation (4) x is expressed in units of cm and b is given in units of cm^{-1}.

Summary of the schematic cloud. The schematic cloud is characterized by Equations(1), (2), (3), and (4). We assumed that the distribution given by Equation (1) was composed of spherical drops in the liquid phase. The distribution is non-zero for $0 \leq a \leq x$ and zero for $a > x$.

Summary of Objectives

The primary objective of this study was to investigate the feasibility of employing a weather radar to obtain precise quantitative measures of the formation of rain in subtropical clouds. The clouds which were studied were of the convective type with rain formation due to droplet growth by coalescence. A secondary objective was to determine the accuracy of the measurement of the vertical velocities associated with the formation of rain. The rate of formation of rain and the vertical velocities are related to changes in the liquid-water content of a cloud. The liquid-water content was measured by a weather radar operating at a wavelength of 10.3 cm. Other parameters which describe the state of a precipitating cloud were related to the power received from the cloud by means of a model. This schematic model is summarized in Equations (1) through (4).

C H A P T E R I I

FORMULATION OF THE CONTINUITY EQUATION

Introduction

The rate of formation and subsequent development of rain in moist air is very closely related to the three-dimensional winds affecting the region of formation. Kessler [1959] has suggested the use of a continuity equation for water substance to gain some insight into changes in cloud parameters. This equation was used by Runnels [1962] and Clark [1964] to calculate vertical speeds in convective clouds. The vertical speeds obtained by this method were reasonable ones for the cumulus congestus clouds that were studied.

If we designate the total concentration of water substance per unit volume in excess of the saturation by M', then a continuous distribution of M' can be represented as a function of the three space coordinates and time; $M' = M'(x,y,z,t)$. The x- and y-directions are horizontal and the z-direction is positive toward the zenith.

The stipulation that M' is the concentration of water substance (water in all its phases) in excess of the saturation value means that M' is essentially the concentration of liquid water, since the degree of supersaturation reached by an ascending parcel of air is small. Supersaturation is rapidly offset by condensation of tiny cloud droplets. Houghton [1951] states that the

maximum value of the supersaturation is reached at the time of activation of the nuclei and thereafter the supersaturation rapidly declines until a condition of quasi-equilibrium is reached, wherein liquid is condensed at the rate dictated by the rate of lift. The theoretical work of Howell [1949], Mordy [1959], and Mason and Chien [1962] demonstrated that the supersaturation seldom exceeds a few tenths of one per cent of the saturation value and then declines to a value of approximately 0.1 per cent.

Since the degree of supersaturation is less than the measurement error of typical humidity sensors, and because the radar measurements used in this study represent averages over several minutes and a volume of several thousand cubic feet of space, it was assumed that condensation occurs at a relative humidity of 100 per cent. With this assumption, M' represents the concentration of condensed water at a point in the atmosphere.

For some point (x,y,z) in the atmosphere, the continuity equation for M' may be written

$$\frac{\partial M'}{\partial t} + \nabla \cdot M'(\hat{C} + V'\hat{k}) = Q, \qquad (5)$$

where C is the three-dimensional wind vector at the point where M' is measured; V' is the effective terminal fall speed of M' relative to the air; $\hat{k}$ is a unit vector which is positive in the direction of increasing z, and Q is a source function which accounts for the local generation or dissolution of M'.

In the work of Kessler [1961], Runnels [1962], and Clark

[1964], the source function was shown to have the following form in saturated air:

$$Q = -\frac{d\rho_s}{dt} = wG_F, \tag{6}$$

where ρ_s is the saturation vapor density and w is the wind speed in the positive z-direction. The quantity, G_F, is termed the "generating function," and is defined as

$$G_F = -\frac{d\rho_s}{dz}. \tag{7}$$

The generating function expresses the amount of liquid condensed from a unit volume of saturated air per unit of vertical distance, and is always a positive quantity. The direction of the vertical speed, w, determines whether the term wG_F represents condensation or evaporation. A positive vertical speed results in condensation while a negative speed produces evaporation at a rate which maintains saturation in a descending parcel.

The primary influence of the generating term is in the generation and subsequent growth by condensation of cloud drops up to a diameter of the order of 50μ. The influence is probably negligible for drops with diameters greater than 100μ [Mason, 1957]. At diameters greater than 100μ, the growth of drops is primarily by coalescence [Langmuir, 1948].

Substitution for Q in Equation (5) and expansion of the vector quantities in terms of their components yields

$$\frac{\partial M'}{\partial t} + \frac{\partial}{\partial x}(M'u) + \frac{\partial}{\partial y}(M'v) + \frac{\partial}{\partial z}(M'w + M'V') = wG_F. \tag{8}$$

Equation (8) may be simplified by using the general equation of

continuity of air,

$$\frac{\partial \rho}{\partial t} = - \rho \nabla \cdot \hat{C} - \hat{C} \cdot \nabla \rho, \tag{9}$$

where ρ is the density of air. The local density change and the horizontal density changes are one to two orders of magnitude smaller than the remaining terms in Equation (9). Neglecting these terms, we will introduce an error of only a few tenths of one per cent to one per cent in the continuity equation. As will be shown later, this error is small compared to the measuring errors encountered in the experiment. With these assumptions, Equation (9) reduces to

$$w \frac{\partial \ln \rho}{\partial z} = - \nabla \cdot \hat{C}. \tag{10}$$

Substitution of Equation (10) into (9) yields

$$\frac{\partial M'}{\partial t} = - u \frac{\partial M'}{\partial x} - v \frac{\partial M'}{\partial y} - w \frac{\partial M'}{\partial z} - \frac{\partial}{\partial z}(M'V') + M' w \frac{\partial \ln \rho}{\partial z} + w G_F . \tag{11}$$

This form of the continuity equation for M' relates the local change of M' to horizontal advection, vertical convection, divergence due to changes of terminal fall speed with height, and condensation in rising air or evaporation in descending air. The term $M'w(\partial \ln \rho / \partial z)$ accounts for the compressibility of the atmosphere.

It was stated in a previous paragraph that the growth of a drop is primarily by condensation when the diameter is less than 100μ and primarily by the coalescence mechanism at diameters

larger than 100μ. This suggests the division of the liquid-water concentration into two sub-concentrations for the purpose of analysis.

The total concentration of water, M', may be thought of as the sum M + m, where M represents the mass concentration of drops whose diameters are larger than 100μ, and m is the mass per unit volume of drops whose diameters are less than 100μ. The sub-concentration represented by M is, essentially, that portion of M' which is detected by radar. In a section to follow, it is shown that a drop diameter of approximately 100μ is the smallest drop size which will produce a detectable signal at the ranges used in this study.

The substitution of M + m for M' in Equation (11) gives

$$\begin{aligned}\frac{\partial M}{\partial t} + \frac{\partial m}{\partial t} = &- u\left[\frac{\partial M}{\partial x} + \frac{\partial m}{\partial x}\right] - v\left[\frac{\partial M}{\partial y} + \frac{\partial m}{\partial y}\right] \\ &- w\left[\frac{\partial M}{\partial z} + \frac{\partial m}{\partial z}\right] - \left[\frac{\partial}{\partial z}(MV_1 + mV_2\right] \\ &+ w\frac{\partial \ln \rho}{\partial z}\left[M + m\right] + wG_f ,\end{aligned} \tag{12}$$

where V_1 and V_2 are the effective terminal fall speeds of M and m respectively and the sum $MV_1 + mV_2$ is the total momentum of the water substance.

The term $\partial(mV_2)/\partial z$ is assumed to be zero since the drops of diameter less than 100μ have no appreciable terminal speed. The drops comprising the concentration represented by m share the vertical speed, w, of the wind and will be termed "cloud."

Since the drops in the sub-concentration designated by M may have fall speeds relative to the updrafts, they will be called "rain." Hereafter, the subscript will be deleted from the symbol V_1 for the sake of simplicity.

Equation (12) may be thought of as the sum of two continuity equations for the sub-concentrations M and m. Since we have considered that the liquid mass represented by M consists of drops with diameters greater than 100μ, then the source term, wG_F, can be neglected at elevations above the cloud base. When we separate Equation (12) into two equations, it is necessary to add a term representing a transfer of mass from the ensemble of small drops to the ensemble of large drops. With these two conditions, Equation (12) may be written as

$$\frac{\partial M}{\partial t} = - u\frac{\partial M}{\partial x} - v\frac{\partial M}{\partial y} - w\frac{\partial M}{\partial z} - \frac{\partial}{\partial z}(MV) + wM\frac{\partial \ln \rho}{\partial z} \qquad (13)$$

$$+ \text{coalescence} - \text{evaporation of rain}$$

and

$$\frac{\partial m}{\partial t} = - u\frac{\partial m}{\partial x} - v\frac{\partial m}{\partial y} - w\frac{\partial m}{\partial z} + wm\frac{\partial \ln \rho}{\partial z} + wG_F \qquad (14)$$

$$- \text{coalescence} + \text{evaporation of rain.}$$

The term "evaporation of rain" accounts for transfer from the large-drop class to the small-drop class as evaporative losses reduce the diameter of a drop to less than 100μ. Subsequent evaporation of the small drops to vapor is taken into account by the source function wG_F.

Ensemble Representations

The verbal terms in Equations (13) and (14) can be understood more clearly if we examine the integral representations of several of the terms in these two expressions. The total liquid-water concentration is given by

$$M' = \frac{\pi}{6} \rho_L \int_0^{x} n(a)a^3 da, \tag{15}$$

the concentration of rain is

$$M = \frac{\pi}{6} \rho_L \int_{a_M}^{x} n(a)a^3 da, \tag{16}$$

and the concentration of cloud is

$$m = \frac{\pi}{6} \rho_L \int_0^{a_M} n(a)a^3 da. \tag{17}$$

The symbols used in Equations (15), (16), and (17) which have not been defined previously are as follows: $n(a)da$ represents the number of drops per unit volume with diameters between a and $a + da$, a_M is the diameter of the smallest drop which will produce a barely-detectable signal at the radar, and x is the diameter of the largest drop in the distribution.

The expressions on the right-hand side of Equations (16) and (17) may be substituted for the quantities M and m respectively in Equations (13) and (14). The term $\partial(MV)/\partial z$ in Equation (13) requires some consideration before a substitution of the integral counterpart is made. The quantity V in this term represents

an average velocity. It is actually an ensemble volume-mean velocity. If the volume-mean velocity is designated by $\langle V \rangle$, it is related to the ensemble terms by

$$\langle V \rangle \int_{a_M}^{\infty} n(a)a^3 da = \int_{a_M}^{\infty} n(a)V(a)a^3 da. \qquad (18)$$

The integral on the left-hand side of Equation (18) is proportional to M. Atlas [1964] has related the volume-mean velocity to the velocity of the drop having the median-volume diameter, a_0. One-half of the total volume of the drops in the M sub-concentration is contributed by drops with diameters greater than a_0. The median-volume diameter is representative for characterizing drop-size spectra. Using drop-size distributions obtained from in-cloud measurements, Atlas [1954] showed that 75 per cent of the energy scattered back to a weather radar is contributed by drops with diameters greater than the median-volume diameter. In the 1964 paper, Atlas states that the ratio $\langle V \rangle / \bar{V}$ is approximately unity for most clouds. The symbol $\bar{V}$ represents the velocity of the drop with the median-volume diameter. The vertical divergence of the flux of rain, therefore, is expressed best as $\partial(M\bar{V})/\partial z$.

Transfer by Coalescence

The integral representation of the coalescence, or ensemble transfer term, follows from derivations presented in works such as those of Johnson [1954], Mason [1957], and Byers [1965].

These writers have shown that the rate of mass increase of a raindrop of diameter α falling at a speed V_α through a cloud of liquid-water content X is given by

$$\frac{dM(\alpha)}{dt} = \frac{\pi\alpha^2}{4} EX[V_\alpha - V_\beta], \tag{19}$$

where V_β is the speed of fall of the small drops of diameter β which make up the cloud. The quantity E is called the collection efficiency, and it indicates the fraction of small drops initially on a collision course with a large drop which actually do collide and coalesce with the large drop.

To derive an integral expression analogous to Equation (19), we need to consider a sub-set of raindrops with diameters between α and $\alpha + d\alpha$ and formulate an expression for the rate of increase of mass in this sub-set due to the coalescences with all other drops. The mass in the sub-concentration M is changed by: (a) coalescence between two drops whose diameters are less than a_M and (b) coalescence between a drop whose diameter is less than a_M and a drop whose diameter is greater than a_M. To simplify the discussion we will designate the drops with diameters less than a_M as "little" drops and drops with diameters greater than a_M as "big" drops.

The drops in the sub-set with diameters between α and $\alpha + d\alpha$ will experience an increase in mass due to coalescences with little drops at a rate given by

$$\delta M = \frac{\pi\alpha^2}{4}\, n(\alpha)d\alpha \int_0^{a_M} \frac{\pi}{6}\rho_L E(\alpha, \beta) n(\beta) \beta^3 [V(\alpha) - V(\beta)]d\beta, \qquad (20)$$

where $n(\beta)$ is the distribution function of the little drops. The rate of transfer of mass per unit volume from the sub-concentration $a<a_M$ to the sub-concentration $a>a_M$ is given by

$$\int_{a_M}^{x} \delta M = \frac{\pi^2 \rho_L}{24} \int_{a_M}^{x} \alpha^2 n(\alpha)d\alpha \int_0^{a_M} E(\alpha, \beta) n(\beta) \beta^3 [V(\alpha) - V(\beta)]d\beta. \qquad (21)$$

The rate of increase of mass due to coalescence between little drops is given by a relation that is similar to Equation (21). However, the mass added to the sub-concentration M is contributed by both of the little drops. The increase of mass in this sub-concentration after the coalescence between a little drop and a big drop results from the mass contributed by the little drops alone. The following expression which represents the increase of mass when two little drops coalesce was suggested by Reid [1965]:

$$\frac{\pi^2 \rho_L}{48} \int_0^{a_M} \alpha^2 n(\alpha)d\alpha \int_\gamma^{a_M} E(\alpha, \beta)(\alpha^3 + \beta^3) n(\beta)[V(\alpha) - V(\beta)]d\beta,$$

where $\gamma^3 = a_M^3 - \alpha^3$. The form of γ assures that the integration involves only little drops whose combined volume is greater than or equal to the volume of a drop of diameter a_M. The sum of this latter integral and the integral given by Equation (21) represents the rate of transfer of mass per unit volume from the sub-concentration m to the sub-concentration M.

The possibility that the larger drops in the sub-concentration M may shatter when $a \gg x$ places a boundary condition on the distribution function, n(a), of the ensemble. The critical diameter for shatter of water drops falling at terminal speed is about 6 mm [Blanchard, 1950]. This boundary condition may be accounted for by assuming that $n(a) \to 0$ as $x \to \infty$ sufficiently rapidly that the fraction of the total mass represented by $a \gg x$ is negligible.

We will show that this condition is satisfied in the case of the M-P distribution. The integral representation of the total liquid-water content with x as an upper limit is

$$M'_x = \frac{\pi \rho_l N_0}{6} \int_0^x \exp(-ba) a^3 da$$

$$= \frac{\pi \rho_l N_0}{b^4} - \frac{\pi \rho_l N_0}{b^4} \left[\exp(-bx) \left(1 + bx + \frac{b^2 x^2}{2} + \frac{b^3 x^3}{6}\right) \right]. \qquad (22)$$

With infinity as an upper limit, the expression becomes

$$M'_\infty = \frac{\pi \rho_l N_0}{6} \int_0^\infty \exp(-ba) a^3 da = \frac{\pi \rho_l N_0}{b^4} . \qquad (23)$$

Values of M'_x, M'_∞, and $M'_\infty - M'_x$ are listed in Table 1 as a function of b and x. The values of b and x in this table are related by the equation

$$x = 9.95 b^{-1.014}$$

The discrepancies between the values M'_x and M'_∞, as listed in the last column in Table 1, show that the M-P distribution function, n(a), does approach zero very rapidly for typical values of b and x. The average discrepancy is 1.46 per cent

Table 1. Variation of the Integral Value of Liquid-water Content as a Function of Various Upper Limits

b	x	M'_x	M'_∞	$M'_\infty - M'_x$	$\frac{M'_\infty - M'_x}{M'_x}$
cm^{-1}	cm	gm m^{-3}	gm m^{-3}	gm m^{-3}	
15	0.64	4.894	4.964	0.070	0.0143
18	0.53	2.360	2.394	0.034	0.0144
21	0.45	1.273	1.292	0.019	0.0149
24	0.40	0.746	0.758	0.012	0.0161
27	0.35	0.466	0.473	0.007	0.0150
30	0.32	0.306	0.310	0.004	0.0131
33	0.29	0.209	0.212	0.003	0.0144
36	0.26	0.147	0.150	0.003	0.0204
39	0.24	0.107	0.108	0.001	0.0093
42	0.22	0.080	0.081	0.001	0.0125
45	0.21	0.060	0.061	0.001	0.0167
					Ave.0.0146

for rainfall rates ranging from very light to heavy (corresponding to values of b varying from 48 cm^{-1} to 15 cm^{-1}, respectively). Therefore, to account for all of the mass in the distribution of water drops, the outer integral in Equation (21) will be evaluated in the limit as $x \to \infty$.

Evaporation

The integral representation of the rate of change of the mass per unit volume due to evaporation in the sub-concentration M can be developed in a manner that is similar to the formulation of the coalescence transfer term. Texts on cloud physics, such as Johnson [1954], Mason [1957], Fletcher [1962], and Byers [1965], show that the rate at which mass is added to a drop of diameter α by condensation, or taken from the drop by evaporation, is given by

$$\frac{dM(\alpha)}{dt} = \frac{\pi \rho_l \alpha}{2} \frac{(S - 1)}{A + B} f(\alpha), \tag{24}$$

where S is the saturation ratio (ratio of ambient vapor pressure to the saturation vapor pressure) and $f(\alpha)$ is the ventilation factor. The ventilation factor is introduced to account for an enhancement of the evaporation or condensation rates as air flows past a drop. The terms A and B have the following meanings:

$$A = \frac{\rho_l L^2}{K R_w T^2},$$

where L is the latent heat of evaporation, K is the coefficient of thermal conductivity, R_w is the specific gas constant for water vapor, and T is the temperature of the drop; and

$$B = \frac{\rho_l R_w T}{D e_s},$$

where D is the diffusivity of water vapor in air and e_s is the saturation vapor pressure.

The rate of change of mass per unit volume, because of evapor-

ation or condensation, of a drop in the sub-set of drops with diameters between α and $\alpha + d\alpha$ is

$$\delta M = \frac{\pi \rho_L}{2} \frac{S - 1}{A + B} \alpha n(\alpha) f(\alpha) d\alpha. \tag{25}$$

The rate of change of mass per unit volume from the sub-concentration in which $a > a_M$ to the sub-concentration $a < a_M$ due to evaporation is

$$\frac{\pi \rho_L}{2} \frac{S - 1}{A + B} \int_{a_M}^{\infty} \alpha n(\alpha) f(\alpha) d\alpha. \tag{26}$$

We stated earlier that the degree of supersaturation in a cloud, during the stage of its growth when coalescence is the dominant effect, is approximately 0.1 per cent. Since this value is less than the measurement errors, the assumption was made that a relative humidity of 100 per cent prevails in the cloud. A relative humidity of 100 per cent corresponds to a saturation ratio of unity, and this, in turn, means the evaporation term in the continuity equation will be zero at altitudes above cloud base.

Summary

With the conditions stipulated in the preceding paragraphs, the two continuity equations (Equations (13) and (14)) reduce to

$$\frac{\partial M}{\partial t} = - u\frac{\partial M}{\partial x} - v\frac{\partial M}{\partial y} - w\frac{\partial M}{\partial z} - \frac{\partial}{\partial z}(M\bar{V}) + wM\frac{\partial \ln \rho}{\partial z} + \tau(a_M) \tag{27}$$

and

$$\frac{\partial m}{\partial t} = - u\frac{\partial m}{\partial x} - v\frac{\partial m}{\partial y} - w\frac{\partial m}{\partial z} + wm\frac{\partial \ln \rho}{\partial z} + wG_f - \tau(a_M). \tag{28}$$

If we confine our study to the center of a convective cloud, Equations (27) and (28) may be written

$$\frac{\partial M}{\partial t} = - w\frac{\partial M}{\partial z} - \frac{\partial}{\partial z}(M\bar{V}) + wM\frac{\partial \ln \rho}{\partial z} + \tau(a_M), \tag{29}$$

and

$$\frac{\partial m}{\partial t} = - w\frac{\partial m}{\partial z} + wm\frac{\partial \ln \rho}{\partial z} + wG_f - \tau(a_M). \tag{30}$$

In these last four equations, $\tau(a_M)$ has been substituted for the integral terms which represent the rate of transfer of mass by coalescence.

When quantities such as $\partial M/\partial t$ and $\partial M/\partial z$ are evaluated from meteorological data, in actuality, the average values of these partial derivatives are obtained for the point in question. Because of turbulent irregularities in the field of M, the ratios $\Delta M/\Delta t$ and $\Delta M/\Delta z$ probably will not approach limiting values, but will oscillate as the increments of time and distance, respectively, are made smaller. Since the radar measurements used in this investigation represent average values over approximately 8 min and 4,000 ft, it was felt that replacement of the partial derivatives in Equations (29) and (30) with finite-difference expressions would produce a more representative equation. After performing these substitutions, we obtain

$$\frac{\Delta M}{\Delta t} = - w\frac{\Delta M}{\Delta z} - M\frac{\Delta \bar{V}}{\Delta z} - \bar{V}\frac{\Delta M}{\Delta z} + wM\frac{\Delta \ln \rho}{\Delta z} + \tau, \tag{31}$$

and

$$\frac{\Delta m}{\Delta t} = - w\frac{\Delta m}{\Delta z} + wm\frac{\Delta \ln \rho}{\Delta z} + wG_F - \tau. \tag{32}$$

CHAPTER III

METHOD OF MEASUREMENT

In this chapter the techniques are developed which were used to estimate the liquid-water content of a cloud. This quantity is not measured directly. Therefore, theoretical expressions are derived which relate the liquid-water content to the radar energy scattered back from a cloud. A description of the weather radar is presented. This is followed by a discussion of the procedure used to convert the directly-measured power to the liquid-water content.

Radar Equipment

The precipitation studied during the course of this investigation was examined with a weather radar operating at a wavelength of 10.3 cm. This radar was constructed at Texas A&M University and is designated the WSR/TAM-1. Moyer [1965] has described some of the recent modifications of this radar, the characteristics of which are shown in Table 2.

Quantitative measurements of received power were made by employing the threshold-gain technique. In this technique, only the received power that exceeds a selected gain-setting of the receiver can modulate the electron beam striking the phosphor of the cathode ray tubes of the radar. To convert a given gain-setting to a particular power value, a calibrating instrument

Table 2. Characteristics of the WSR/TAM-1 Radar

Transmitted power	180 kw
Pulse repetition frequency	186 sec^{-1}
Wave length	10.3 cm
Pulse length (time units)	5.0 μsec
Pulse length (length units)	1.5×10^{3}m
Antenna shape	Paraboloidal
Antenna diameter	4.572 m
Antenna gain	8.0×10^{3}
Horizontal beam width	1.60 deg
Vertical beam width	1.60 deg
Minimum detectable signal	1.3×10^{-14}w
Antenna elevation (MSL)	413 ft

is employed. A Webster-Chicago TS 155E/UP signal generator was used to calibrate the TAM-1 radar. The calibration procedure consisted of recording the power output of the signal generator which barely exceeded a threshold determined by the bias voltage of the receiver-gain control. Each decremental step of the gain-stepping device was related to a definite value of bias voltage, and, therefore, was equivalent to a value of power from the signal generator. If an echo was present at a given gain-step and not present at the next higher step, the received power was taken to be the value in decibels below one milliwatt (dbm)

corresponding to the mid-point between the two gain-steps. This technique introduces an uncertainty of half a gain step in the values of received power.

The receiver gain was changed in discrete steps by a control which was actuated by the rotation of the antenna. The gain was changed at a rate of one step for each revolution of the antenna. The data were recorded on 35-mm film by a Fairchild radarscope camera attached to one of the Plan-Position Indicator (PPI) oscilloscopes. One frame of film was exposed for each revolution of the antenna, and, as a consequence, one frame was exposed for each gain-step setting.

Procedure

Radar equation. The power received from a meteorological target can be related to characteristics of the target by using a form of the principle of conservation of energy. The form of this principle, which is applicable to meteorological targets, is termed the "radar equation." Derivations of this equation are given by Kerr [1951], Battan [1959], and Probert-Jones [1962]. The form developed by Probert-Jones is a modification of the equations given by Kerr and Battan and is a more precise version. Calculations of the power expected from a given rainfall rate, which were based on the form of the equation prior to the Probert-Jones development, were consistently in error by amounts ranging up to 7 dbm. Error analyses indicated

that the error was systematic in nature. Probert-Jones was able to show that a part of this systematic error was due to faulty assumptions concerning the effective width of the radar beam. These assumptions caused users of the equation to overestimate both the antenna gain and the volume illuminated by the radar beam. Using a theoretical shape of the radar beam which was more realistic, Probert-Jones was able to reduce the systematic overestimate to 1.4 dbm. The remaining error probably results from the inexactness of the expression that relates rainfall rates to received power and to the shape assumed for the beam.

If there is no significant attenuation of the radar energy between the radar and the target and the volume illuminated by the beam is uniformly filled by the target, then the Probert-Jones equation relates the average power, $\bar{P}_r$, received from a scattering volume at a slant range r to characteristics of the volume and the radar by

$$\bar{P}_r = \left[\frac{P_t G^2 \lambda^2 h \theta \varphi}{1024 \pi^2 \ln 2}\right] \frac{1}{r^2} \int_{a_M}^{\infty} n(a) \sigma(\lambda, a, T) da. \qquad (33)$$

The terms within the brackets are characteristic of any given radar and may be combined into a term C, that is constant for that radar. The parameters that make up this radar constant are P_t, the transmitted power, G, the antenna gain, λ, the wavelength of the radar, and θ and φ, the horizontal and vertical beam widths to half-power points, respectively. The radar constant

for the TAM-1 has been evaluated from the data in Table 2, and has a value of 8.344×10^6 mw mi^2 cm.

The integral expression in Equation (33) is a measure of the efficiency of the radar target in intercepting radio energy and returning it to the radar receiver. Traditionally, this quantity has been termed "radar reflectivity" and designated by the symbol η. As is indicated by the terms in the integrand, the radar reflectivity depends on the drop-size distribution and the number of drops per unit volume (indicated by n(a)), the wavelength of the radiation interacting with the drop, the diameter of the drop, and the temperature, T, of the drop. The parameter σ is called the radar cross section or back-scattering cross section. A consideration of the integral expression shows that η represents the summation over a unit volume of the back-scattering cross sections of the individual drops.

The radar cross section is defined by Kerr [1951] as "the area intercepting that amount of power which, when scattered isotropically, produces an echo equal to that observed from the target." This cross-section is a convenient quantity for describing the variability of the interaction between a plane electromagnetic wave and a "scattering" object. A general treatment of the problems of scattering of a plane wave by a sphere of any size and various electrical properties was made by Mie [1908]. Additional research related to the scattering problem has been performed by several workers since the time of Mie's paper

[Aden, 1952]. The Mie theory describes the back-scattering cross section in terms of an infinite series of spherical Bessel functions. Detailed discussions of the rigorous solution of Mie are given by Von [1963] and Greene [1964] who followed the technique of Aden [1952]. Because of the complicated nature of coefficients in the Mie solution, the simpler theory of Rayleigh has been used to explain scattering when the radius of the scatterer is less than approximately one-tenth the wavelength of the incident radiation. The Rayleigh theory adequately describes the scattering properties of raindrops of diameters less than about 0.35 cm when these drops are illuminated with 10.3-cm radiation.

The average received power is specified in Equation (33) since we are measuring the power scattered from a random distribution of drops within a pulse volume. It is the average power only which is related to the radar reflectivity of a random array of scatterers [Atlas, 1964].

As given, Equation (33) is applicable to the situation in which there is no significant attenuation of the radar energy between the radar and the target, and the volume illuminated by the beam is uniformly filled by the target. The condition of negligible attenuation is satisfied for wavelengths of 10 cm or greater. Equation (33) can be used, therefore, to relate the received power measured with the TAM-1 radar to a meteorological target if the second condition, regarding beam filling, is met. According to Donaldson [1965], errors resulting from the failure

of a precipitating volume to completely fill the radar beam can be held to less than the errors in the measurement of the received power if the product of the range (in nautical miles) and the beam width (in degrees) to half-power points is less than 50. For the TAM-1 radar, with a beam width of 1.6 deg, the condition of the beam being uniformly filled with scatterers is satisfied to a high degree of accuracy if the precipitation echoes chosen for study are within a range of 36 st mi from the radar. A complete discussion of errors inherent in the use of Equation (33) appears in Chapter IV.

The radar equation may be expressed in a more compact form by using the symbols mentioned earlier. With C representing the radar constant and η standing for the total back-scattering cross section per unit volume, Equation (33) may be written as

$$\bar{P}_r = \frac{C\eta}{r^2} . \tag{34}$$

Liquid-water content. To calculate the rate of transfer of liquid-water from the sub-concentration m to the sub-concentration M, a method is needed to convert the radar reflectivity, η, to a value of water mass per unit volume. In this section an expression will be derived which relates these two quantities.

The liquid-water content, M, which is observed by the radar, is related to the drop-size distribution by

$$M = \frac{\pi \rho_L}{6} \int_{a_M}^{\infty} n(a) a^3 da. \tag{35}$$

For the M-P distribution, Equation (35) becomes

$$M = \frac{\pi N_0}{6} \int_{a_M}^{\infty} \exp(-ba) a^3 da. \tag{36}$$

The density of the drops, ρ_L, has been omitted from Equation (36) since it is assumed to be unity in the cgs system.

For the M-P distribution, the radar reflectivity has the form

$$\eta = N_0 \int_{a_M}^{\infty} \exp(-ba) \sigma(a, \lambda, T) da. \tag{37}$$

The Mie back-scattering cross section is the analytical form which most accurately represents the empirical values determined under laboratory conditions. These back-scattering cross sections are difficult to use because of complicated form of the coefficients in the Mie solution. Von et al. [1964] have shown that the back-scattering cross section of Mie, σ_M, can be related to the simpler back-scattering cross section of Rayleigh, σ_R, by

$$\sigma_M / \sigma_R = F(\lambda, a, T), \tag{38}$$

where $F(\lambda, a, T)$ is a polynomial which was fitted by the method of least squares to the curves of the ratio σ_M / σ_R. A quadratic equation, accurate to a few per cent, easily fitted the 10.3-cm data. Substitution of σ_M from Equation (38) for the quantity σ in Equation (37) gives

$$\eta = N_0 \int_{a_M}^{\infty} \exp(-ba) F(\lambda, a, T) \sigma_R da. \tag{39}$$

The Rayleigh approximation to the Mie back-scattering cross

section is given by

$$\sigma_R = \frac{\pi^5}{\lambda^4} \left| \frac{\epsilon^2 - 1}{\epsilon^2 + 2} \right|^2 a^6, \tag{40}$$

where ϵ is the complex index of refraction. For the sake of simplicity, we shall designate the quantity $|(\epsilon^2 - 1)/(\epsilon^2 + 2)|$ by K. Elimination of σ_R between Equations (39) and (40) gives

$$\eta = \frac{\pi^5}{\lambda^4} K^2 N_0 \int_{a_M}^{x} \exp(-ba) a^6 F(\lambda, a, T) da. \tag{41}$$

The radar reflectivity for the simpler case of Rayleigh scattering is

$$\eta = \frac{\pi^5}{\lambda^4} K^2 N_0 \int_{a_M}^{x} \exp(-ba) a^6 da. \tag{42}$$

If we designate the radar reflectivity applicable to Rayleigh scattering as η_R and compare this to the Mie value, as given by Equation (41), we obtain

$$\frac{\eta}{\eta_R} = \frac{N_0 \int_{a_M}^{x} \exp(-ba) a^6 F(\lambda, a, T) da}{N_0 \int_{a_M}^{x} \exp(-ba) a^6 da} \tag{43}$$

The denominator of the right-hand side of Equation (43) is usually termed the "reflectivity factor" and designated by Z. The ratio η/η_R was shown by Stephens [1964] to be a function of b and x and to vary only slightly with temperature at 10.3 cm. Indicating this function by f(b,x), we can rearrange Equation (43) and get the following relation between Z and η:

$$Z = \frac{\eta\lambda^4}{\pi^5 K^2} \frac{1}{f(b,x)}. \qquad (44)$$

It was desirable to convert the values of η, as computed from the measured values of $\bar{P}_r$, to values of Z since the reflectivity factor has a much simpler mathematical form.

We showed in Chapter I that the data collected at a sub-tropical location indicate that b and x are related for typical rates of rainfall. Therefore, in the case of the schematic sub-tropical cloud of this study, f can be expressed as a function of x or b alone. The variation of f as a function of b, with $x = 9.95b^{-1.014}$, is shown in Figure 1.

The data of Figure 1 indicate that the reciprocal of f differs slightly from unity. The value of 1/f varies from 1.005 (corresponding to b = 42) to 1.092 (corresponding to b = 15). The error encountered in neglecting the factor 1/f in Equation (44) is less than the experimental error involved in the measurement of η. With f assumed to be unity, the elimination of η between Equations (34) and (44) gives

$$\bar{P}_r = \frac{C_1 K^2 Z}{r^2}, \qquad (45)$$

where

$$C_1 = \frac{\pi^5 C}{\lambda^4}.$$

For the TAM-1, C_1 has a value of 2.268×10^{-6} mw $mi^2 m^3 mm^{-6}$.

Since M is proportional to a^3 and Z is proportional to a^6, an expression that relates M to Z will be one in which Z is

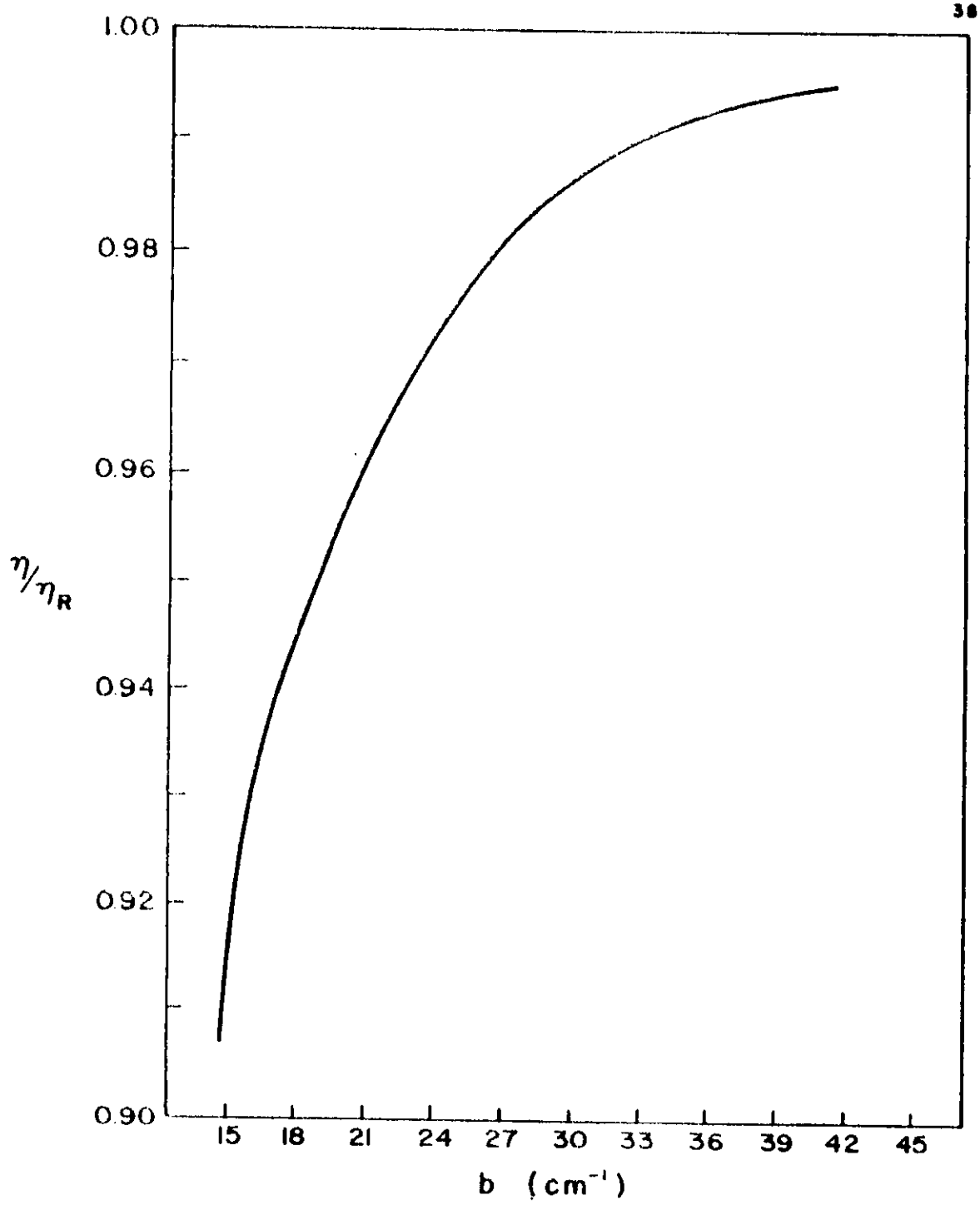

FIG 1. THE VARIATION OF η/η_R WITH b [ADAPTED FROM STEPHENS (1964)].

approximately proportional to the square of M. Battan [1959] has listed the results of empirical studies that compared the liquid-water content and reflectivity factor for observed rates of rainfall and drop-size data. A relationship between Z and M that was derived from data analyzed by Marshall and Palmer [1948] and is representative of most rains is

$$Z = 2.39 \times 10^{4} M^{1.82}. \tag{46}$$

In Equation (46) Z is expressed in $mm^6 m^{-3}$ and M in gm m^{-3}. Liquid-water content can be related to received power by combining Equations (45) and (46). Elimination of Z between these two equations gives

$$M = 3.94 \times 10^{-3} \left[\frac{\bar{P}_r r^2}{C_1 K^2}\right]^{0.55} . \tag{47}$$

Equation (47) is the basic relation that was used in this study to relate the liquid-water content of a volume of rain drops at a given range to the received power that was measured by the TAM-1 radar.

An estimate of the systematic error incurred in using Equation (47) can be obtained by considering the equation

$$\bar{P}_r = \frac{C_2 R^{1.6}}{r^2} , \tag{48}$$

where R is rainfall rate and C_2 is a constant. This equation is the result of combining Equation (45) with the empirical relation $Z = 200R^{1.6}$. This latter expression is most commonly used for rains. Probert-Jones [1962] showed that the values of received

power computed from Equation (48), for a given rainfall rate and range, were larger than the measured values by 1.4 dbm. The error arises from faulty assumptions regarding factors that make up the constant C_2. If the calculated values of $\bar{P}_r$ are too large, then the value of C_2 is too large. Solving Equation (48) for R, we get

$$R = \left[\frac{\bar{P}_r r^2}{C_2}\right]^{0.625} . \qquad (49)$$

If C_2 is too large, then rainfall rates computed from this equation are too small. Since Equation (47) is of the same form as Equation (49), it follows that the values of M computed from Equation (47) will be too small. The order of magnitude of the error in Equation (47) is about the same as the error in Equation (49) since both M and R are proportional to a^3. It seems reasonable to assume that a systematic error of 1.4 db is incurred when Equation (47) is used.

Diameter of the smallest drop capable of detection by radar. The evaluation of the integral terms in Equation (27), the continuity equation, will give theoretical values of the rate of transfer of liquid water due to coalescence. These values may then be compared with rates of transfer determined from the substitution of experimentally-measured quantities into the continuity equation. In Chapter II we showed that a suitable lower limit for this integral would be of the order of 100μ. To insure that the sub-concentration M, as detected by the radar, will consist of

drops of diameter greater than 100μ, the detection capabilities of the TAM-1 radar must be considered.

The smallest rain drop which can give a detectable radar signal is not easily determined from radar measurements. A single drop may not scatter sufficient energy to be detected, but a large number of these same drops may scatter enough energy in the direction of the radar to give a measureable signal.

The radar equation may be used to compute the values of the reflectivity factor, Z, corresponding to a barely-detectable signal at a specified range from the radar receiver. Solution of the radar equation of Z gives

$$Z = \frac{\bar{P}_r r^2}{C_1 K^2}. \tag{50}$$

If the smallest value of the received power that can be detected by the radar, above the circuit noise, is inserted for $\bar{P}_r$ in Equation (50), these minimum values of Z can be calculated as a function of range. The minimum detectable signal for the TAM-1 radar is 1.3×10^{-14}w. The values of Z computed from Equation (50), with $\bar{P}_r = 1.3 \times 10^{-14}$w, are shown as a function of range in Figure 2.

Two principal interpretations are used to convert these minimum values of Z to the size of a drop that is barely detectable. Atlas [1954] stated that the best answer to the question of a smallest drop, detectable by radar, is the median-reflectivity diameter, a_{50}. One-half of the total reflectivity factor is

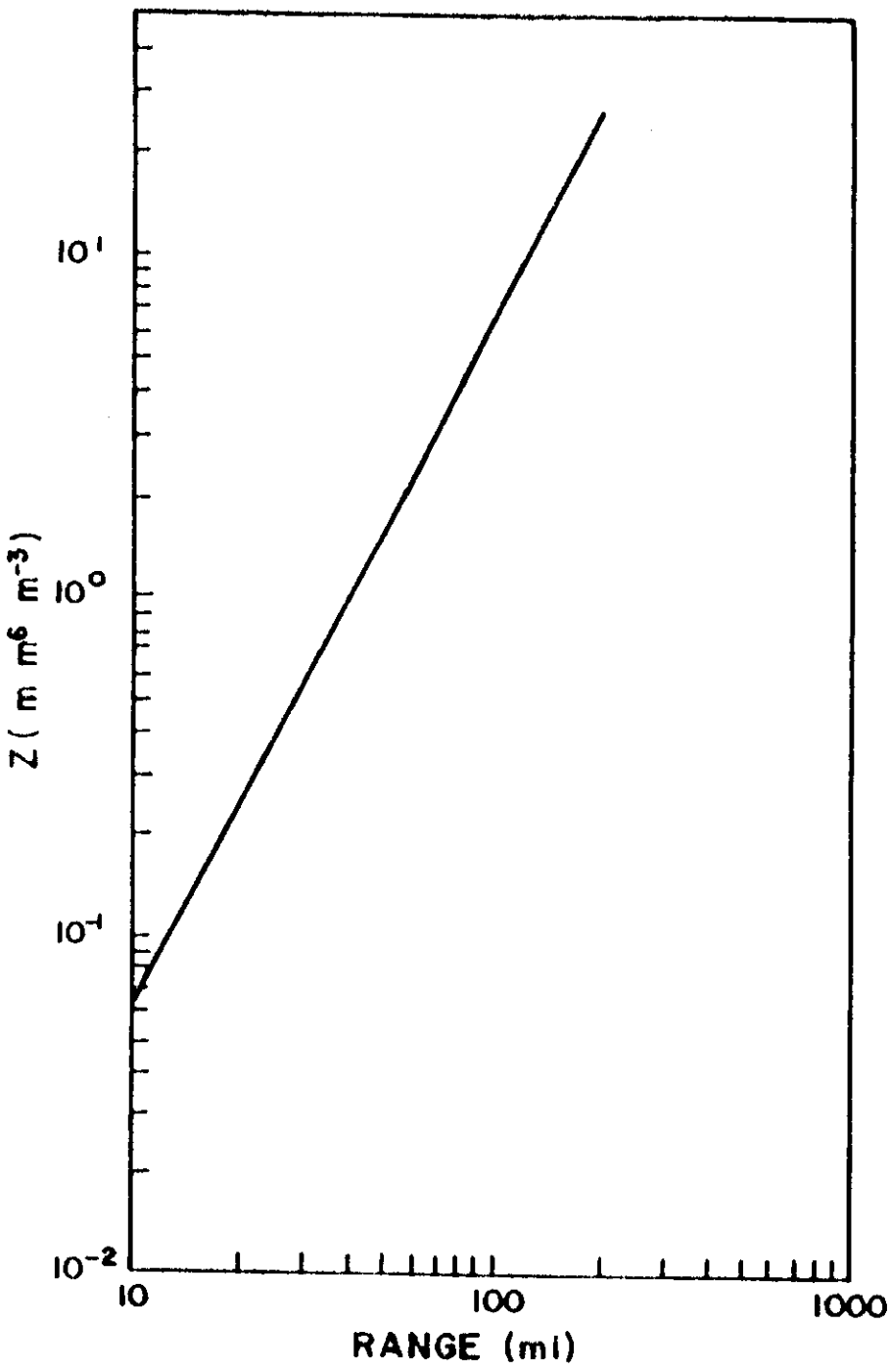

FIG. 2. VALUES OF Z THAT WILL GIVE A BARELY DETECTABLE SIGNAL AT VARIOUS RANGES FROM THE TAM-I RADAR.

contributed by drops with diameters greater than a_{50}. Atlas computed the ratio of a_{50} to a_0 for in-cloud data and obtained the average ratio $a_{50}/a_0 = 1.17$. The cloud data were from six types ranging from stratocumulus to cumulus congestus. Using the Atlas interpretation of a smallest-detectable drop, we note that this drop has a size that is slightly larger than the median-volume diameter.

The other approach to the interpretation of these minimum values of Z in terms of a drop size considers a size distribution in which all of the drops are of the same diameter. Such a distribution is referred to as monodisperse.

The reflectivity factor for a monodisperse distribution is simply

$$Z = Na^6, \tag{51}$$

where N is the total number of drops in a unit volume, all with a diameter a. A drop diameter can be computed for values of Z and N. The values of Z, of course, will be the minimum ones as range varies. The dependency on N can be eliminated by using the liquid-water content. The liquid-water content of a monodisperse distribution is given by

$$M = \frac{\pi}{6}\rho_L Na^3. \tag{52}$$

Elimination of N between Equations (51) and (52) gives

$$Z = \frac{6Ma^3}{\pi\rho_L}. \tag{53}$$

Substitution for Z from Equation (50) and use of the minimum detectable power, $\bar{P}_{min}$, yield

$$a_M^3 = \frac{\bar{P}_{min} \pi \rho_L r^8}{6 C_1 K^2 M} , \tag{54}$$

where a_M is the diameter of the smallest drop which will produce a barely-detectable signal at the radar. Figure 3 shows a_M as a function of liquid-water content and the range for the TAM-1 radar.

The assumption of a perfectly monodisperse distribution is inappropriate in nature, but the values calculated by this method serve to give the order of magnitude of the drop diameter required for detection. The choice of the median-reflectivity diameter, as proposed by Atlas, appears to be a more unsatisfactory one than is the selection of the diameter of a drop in a monodisperse distribution. The median-reflectivity diameter, by its definition, is not the smallest size which can be detected by a radar. One-half of the contribution to the total reflectivity is made by drops with diameters less than a_{50}.

Summary of the procedure. Point estimates of liquid-water content were made by measuring the power received from a volume of convective cloud. The values of received power were converted to values of liquid-water content by employing Equation (47). A systematic correction was applied to these values to account for inexactness in this expression. A minimum range of 30 st mi was chosen to satisfy the condition that only drops with

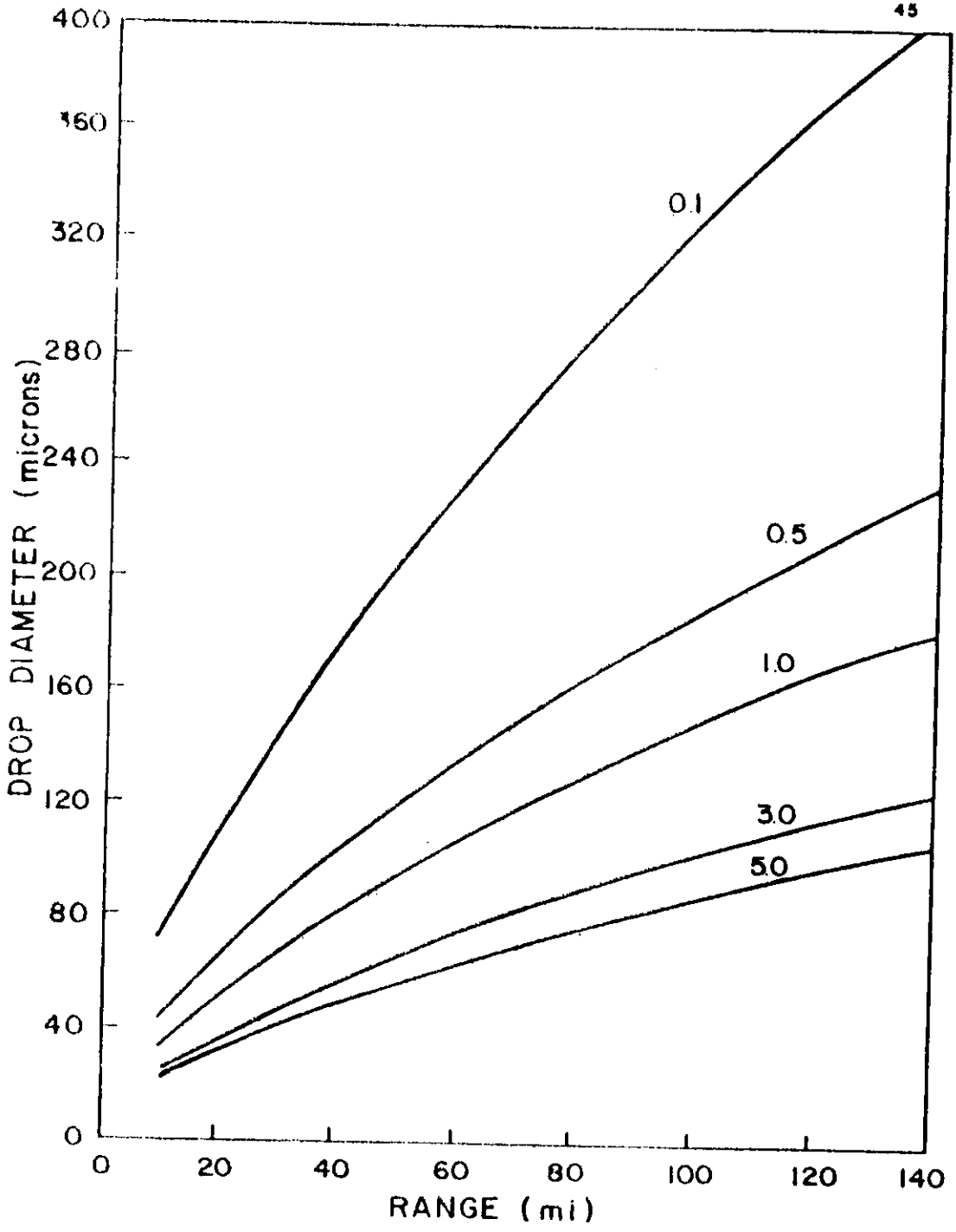

FIG. 3. SIZE OF THE DROPLETS REQUIRED TO GIVE DETECTABLE SIGNALS AT VARIOUS DISTANCES FROM THE TAM - I RADAR. ISOPLETHS ARE LIQUID - WATER CONTENT IN GM M^{-3}

diameters of the order of 100μ and larger were being detected by the radar.

CHAPTER IV

ERROR ANALYSIS

The analysis which was performed to estimate the errors of measurement is discussed in this chapter. The uncertainty in the measurements of the liquid-water content is considered first and this is followed by an examination of the errors that are introduced when the continuity equation is used.

Liquid-Water Content

Over-all error. The liquid-water content for a point within a cloud was shown to be related approximately to the average received power by the expression

$$M = 3.94 \times 10^{-3}\left[\frac{\bar{P}_r r^2}{C_1 K^2}\right]^{0.65} . \qquad (47)$$

We stated in Chapter III that this equation probably underestimates the liquid-water content because of an inexact description of the radar beam. A reasonable estimate of the uncertainty can be made if C_1 is determined from the version of the radar equation derived by Probert-Jones [1962]. Using his expression for C_1 and assuming Rayleigh scattering, we accounted for the systematic underestimate of M by increasing the measured values of $\bar{P}_r$ by 1.4 db.

Calculation of the error of $\bar{P}_r$. The received power was measured by using the threshold-gain technique. The gain setting

of the receiver was varied by discrete steps. We mentioned in Chapter III that the received power was interpreted as the power value in db corresponding to the mid-point between two gain steps if a signal was recorded at one step but was absent at the next. The estimated value of the received power could be in error by as much as 2 db on either side of the mid-point value. This technique therefore introduced an uncertainty of $\pm$ 2 db in the measured values of $\bar{P}_r$ since gain-step decrements of 4 db were used for the TAM-1 radar. This error was brought about by the size of the scale division (gain-step decrement) used. Reduction of this decrement would improve the accuracy of the measurements.

When the threshold-gain technique is used, a systematic error arises that is specific to this method. A threshold signal implies a minimum of integration. In the ideal case, one pulse exceeding the threshold power may be sufficient to give a detectable signal. As the radar beam scans across a cloud, several pulses of transmitted power will, in general, illuminate the most reflective part of the cloud. There is a good chance that one of the returned pulses will contain sufficient power to exceed the threshold level by a considerable amount [Atlas, 1964]. If this pulse is detected as a threshold signal, the average received power will be overestimated. Atlas [op.cit.] states that the strength of the precipitation echo, when estimated by the threshold-gain technique, is too great by some 5 to 6 db.

When photographs are made of the cathode-ray tube (CRT)

of the receiver, two types of systematic errors are encountered which cause underestimations of the received power. One error arises because the threshold for the CRT phosphor exceeds the gain threshold by about 2 to 3 db [Atlas, op.cit.]. The other error concerns the threshold of the film used to record the signal. Clark [1964] reported that the threshold of the film was about 2 db greater than the eye threshold. These two errors will make it appear that the receiver gain has accomplished complete attenuation of a signal at a lower gain-step than would be the case if these systematic errors were not present. Since we were using the photographic technique to record the values of $\bar{P}_r$, these two systematic errors would cause us to calculate a value of $\bar{P}_r$ that is lower than the actual value by 4 to 5 db.

The magnitudes of the three systematic errors indicate that the two errors causing an underestimation of received power essentially compensate for the overestimation which results from employing the threshold-gain method. Therefore, these errors were not considered in the determination of the over-all systematic error.

Two additional errors which contributed to the total error of $\bar{P}_r$ were those due to calibration and experimental conditions. It is estimated that the signal generator which was used to calibrate the gain-steps is accurate to 1 db. Day-to-day variations in the settings of the bias voltage will cause errors in the estimation of the gain-steps. We estimated an error of

1 db in the received power because of varying experimental conditions [Clark, op.cit.].

The total error encountered in measuring the average received power is the result of uncertainties in estimating the gain-step, calibration errors, and variations in the experimental conditions. Therefore, the total error of $\bar{P}_r$ is estimated to be ± 4 db.

Estimation of the error of r and K^2. The range error was estimated to be of the order of ± 2.0 mi. The dielectric factor, K^2, varies with the phase of the water drops. To insure that only liquid drops were being illuminated, only the portions of the echoes which were at altitudes less than 20,000 ft were studied. Therefore, a value of K^2 equal to 0.933, which is appropriate to liquid-water, was used in Equation (47). Based on data reported by Clark [op.cit.], this value may vary by ± 0.003 for temperatures between -8C and 20C. It was assumed that K^2 was in error by ±0.003.

Calculation of the error of C_1. The modified radar constant, C_1, is related to the characteristics of the TAM-1 by

$$C_1 = \frac{P_t G^2 \theta^2 h \pi^3}{\lambda^2 1024 \ln 2} \qquad (55)$$

Estimates of the uncertainties in the parameters on the right-hand side of Equation (55) were made after consultation with Dr. Robert A. Clark, Associate Professor, and Mr. Jake Canglose, Weather Radar Engineer, of the Department of Meteorology of

Texas A&M University. The determination of the total error of C_1 was based on the methodology that is variously called "compounding of errors" [Wilson, 1952] or "propagation of errors" [Beers, 1957]. Calculation of the error is summarized in Table 3.

Table 3. Summary of the errors of C_1

Parameter	Fractional Error	Power	Magnitude of Contribution	Square of Contribution
P_t	0.278	1	0.278	0.0773
G	0.412	2	0.824	0.6790
h	0.100	1	0.100	0.0100
θ	0.312	2	0.624	0.3894
λ	0.011	-2	0.022	0.0005
			Total	1.1562
The fractional error of C_1 is $\sqrt{1.1562}$ =				1.075.

The figures in the column headed by the word "power" correspond to the exponents of the variable terms in Equation (55). The product of the fractional error and the absolute value of the "power" gives the magnitude of the contribution to the total error by the parameter in a particular row. The form of Table 3 was chosen to facilitate the computation of the error of C_1. When the parameter being considered is the product of factors raised to various power, the fractional error of that parameter is equal to the square root of the sum of the terms consisting of the squares of the fractional errors of the constituent

quantities multiplied by the squares of their respective powers.

The absolute error of C_1 is the product of the fractional error and the value of C_1. Multiplication of these two quantities gives 2.545×10^{-8} mw mi^8 m^3 mm^{-6}. The estimated value of the absolute error of C_1 is rather large in comparison to the computed value of C_1; specifically 2.368×10^{-8} mw mi^2 m^3 mm^{-6}. The largest contributions to the error of C_1, as shown in Table 3, were due to the measurements of the gain and the beam width. Since each of these quantities appears to the second power in Equation (55), the errors in these two terms are the predominant contributors to the total error. Any improvements in the accuracy of C_1 would have to be obtained by improving the measurements of G and θ until their uncertainties were comparable to the errors of P_t, h, and λ. Further improvement would require reduction of the errors of all the quantities which make up the radar constant.

Calculation of the error of M. A method similar to the one used to compute the error of C_1 was used to evaluate the error of the liquid-water content. Calculation of the fractional error of M is summarized in Table 4.

The errors of the received power and the radar constant were the largest contributors to the error of M. The error of the radar constant was discussed in a previous paragraph. Of the total error of the received power, the uncertainty arising from use of the gain step method is the greatest. Reduction of

Table 4. Summary of the error of M

Parameter	Fractional Error	Power	Magnitude of Contribution	Square of Contribution
$\bar{P}_r$	1.512	0.55	0.832	0.692
C_1	1.075	-0.55	0.591	0.349
r	0.080	1.10	0.088	0.008
K^2	0.003	-0.55	0.002	0.000
			Total	1.049
The fractional error of M is $\sqrt{1.049}$ =				1.024.

this 2-db error would have to be made before any improvement would be realized in the error of the liquid-water content.

Continuity Equation

The average vertical speed, w, was shown to be related to the rate of change and vertical gradient of M by

$$w = \frac{\frac{\Delta M}{\Delta t} + M\frac{\Delta \bar{V}}{\Delta z} + \bar{V}\frac{\Delta M}{\Delta z} - r}{M\frac{\Delta \ln \rho}{\Delta z} - \frac{\Delta M}{\Delta z}} . \qquad (56)$$

The fractional error of the vertical speed, w, is equal to the square root of the sum of the squares of the fractional errors of the terms on the right-hand side of Equation (56). Therefore, the fractional error of w, S_w, is given by

$$S_w = (S_1^2 + S_2^2 + S_3^2 + S_4^2 + S_5^2 + S_6^2)^{\frac{1}{2}}, \qquad (57)$$

where the subscripts 1 through 6 refer to the terms on the right-hand side of Equation (56). The numbering proceeds from

left to right in the numerator and then from left to right in the denominator. Thus the error of $M(\Delta \ln \rho/\Delta z)$ is designated by S_5.

Partial errors. The method of calculating the fractional error of the terms in the continuity equation was similar for each of the terms since all but one is expressed as a ratio. We will show the development of the error of $\Delta M/\Delta t$ and simply state the calculated errors of the remaining terms.

The error of $\Delta M/\Delta t$, S_1, is

$$S_1 = (S_{\Delta M}^2 + S_{\Delta t}^2)^{\frac{1}{2}}, \tag{58}$$

where $S_{\Delta M}$ is the error of ΔM and $S_{\Delta t}$ is the error of Δt. The error of the time increment was very small since the clock used to measure time varied only in a slow systematic manner. The absolute error of ΔM, $s_{\Delta M}$, is related to the absolute error of M, s_M, by

$$s_{\Delta M}^2 = 2\, s_M^2. \tag{59}$$

The absolute error of M may be expressed as

$$s_M = S_M\, M, \tag{60}$$

where M is evaluated at the center of the difference ΔM. Elimination of s_M between Equations (59) and (60) gives

$$s_{\Delta M}^2 = 2\, S_M^2 M^2,$$

and division by $(\Delta M)^2$ yields

$$S_{\Delta M}^2 = 2\, S_M^2 \left(\frac{M}{\Delta M}\right)^2. \tag{61}$$

Equation (61) shows that the fractional error of ΔM depends on the time and location in the cloud at which M and ΔM are measured. To determine an upper limit of $S_{\Delta M}$, it was decided to choose a value of M corresponding to a reasonably-large value that could be expected in the clouds which were studied. The summary of the maximum values of liquid-water content that is given in the text by Fletcher [1962] was used to ascertain this large value. A value of 2.0 gm m^{-3} appeared to be an average of the various maxima that appeared in the summary. For a value of ΔM to be used in Equation (61) we decided to use a small, yet representative, value of ΔM in order to obtain a value of the error which is unlikely to be exceeded by any one measurement. A value of 0.3 gm m^{-3} appeared to be a typical minima of the values calculated during a case study using the TAM-1 radar. Substitution of the above-mentioned values for M and ΔM into Equation (61) gives

$$S_{\Delta M} = 9.34\ S_M$$
$$= 9.656,$$

which is the same as the fractional error S_1.

The error of $M(\Delta\bar{V}/\Delta z)$ was determined in a manner which is similar to the method used above. The square of the fractional error of M was added to the squares of the errors of $\Delta\bar{V}$ and Δz. The fractional error of Δz is small since the difference of two heights of the center of the radar beam is being considered. The random errors encountered in measuring the height of the radar beam are small and any systematic error will be compensating when

differences in height are considered. It was estimated that the fractional error of $\Delta\bar{V}$ was small compared to the rather large error of M. With these assumptions the fractional error of $M(\Delta\bar{V}/\Delta z)$ was estimated to be 1.024.

Since the term $\bar{V}(\Delta M/\Delta z)$ contains the same parameters as $M(\Delta\bar{V}/\Delta z)$, the error of the former term was estimated to be 1.024.

The fractional error of $\Delta M/\Delta z$ is essentially the error of ΔM since Δz has a very small uncertainty compared to the uncertainty in ΔM. We showed in a previous paragraph that the fractional error of ΔM is 9.656.

The error of τ cannot be determined with great certainty since in-cloud comparisons are not available. The factor causing the greatest uncertainty in τ is the form of the drop-size distribution. Wexler [1948] has estimated that a failure to characterize properly the drop-size distribution may produce errors in the liquid-water content by as much as a factor of two. It seems reasonable to assume an error that is no greater than the errors of the other terms in the continuity equation. With this assumption, the fractional error of τ is roughly estimated to be 2.0.

Previous work by Runnels [1962] and Clark [1964] showed that the term $\Delta(\ln\rho)/\Delta z$ differs very slightly from a constant value. The error encountered by assuming $\Delta(\ln\rho)/\Delta z$ = constant is very small compared to the error of M. Therefore, it was assumed that the fractional error of $M\Delta(\ln\rho)/\Delta z$ was essentially the error of M, i.e., 1.024.

During the development of the continuity equation several terms were neglected since they are small in comparison with the other quantities. Table 5 lists these terms together with the corresponding error that will be introduced if these terms are neglected.

Table 5. Summary of additional errors in the continuity equation

Quantity	Error
$\frac{\partial \rho}{\partial t}$	1%
$\frac{\partial \rho}{\partial x}$	1%
$\frac{\partial \rho}{\partial y}$	1%
S	0.1%
$\frac{\partial M}{\partial x}, \frac{\partial M}{\partial y}$	Negligible[1]

These errors are very small and their contribution to the total error of w was negligible. Therefore, we have not considered these errors in the computation of the total error of w.

[1] Atlas and Banks [1951] estimated that the echo pattern differs very slightly from the isohyetal pattern for wavelengths greater than 7 cm if the range is greater than twice the depth of the echo.

Calculation of the total error of w. Equation (57) was used to compute the total error of w. The values of the partial errors, which are discussed in the above paragraphs, were substituted for the terms on the right-hand side of the equation. Table 6 summarizes the calculation of the error of w.

Table 6. Summary of errors of w

Term	Error	Square of error
$\frac{\Delta M}{\Delta t}$	9.656	93.238
$\bar{V}\frac{\Delta M}{\Delta z}$	1.024	1.048
$M\frac{\Delta \bar{V}}{\Delta z}$	1.024	1.048
τ	2.000	4.000
$M\frac{\Delta(\ln \rho)}{\Delta z}$	1.024	1.048
$\frac{\Delta M}{\Delta z}$	9.656	93.238
	Total	193.620
Square root of total =		13.914

The fractional error of w, therefore, is estimated to be ± 13.914 (a percentage error of ± 1391.4%) and the error in decibels is ± 11.74 db.

Reduction of this error would require reductions in the

error of M since the error of the measurements of liquid-water content is the largest contributor to the error of w.

Meaning of the Estimates of the Error

The previous discussions of the estimated limits of the errors of M and w have considered quantitative measures of these uncertainties, but a precise meaning of the error limits was not considered. In this section a discussion is presented concerning the nature of the experimental error.

In a previous paragraph we stated that semi-objective estimates were made of the error limits of the parameters which appeared in the basic equations. These estimates are termed semi-objective since they represent estimates that were not determined with a degree of accuracy necessary for a rigorous analysis of the experimental errors. However, it was felt that these estimates were the best available and that the magnitudes were reasonable ones.

Before assigning a specific meaning to these semi-objective estimates, we will consider the nature of the observations which determine the form of the quantity used to express the limits of error. These forms are based on the assumption that successive observations of the same quantity should be distributed in a random sequence. It is considered that there exists a hypothetical population made up of the results which would be obtained if the given observation were repeated a very large number of times.

Any single observation or set of observations is regarded as a random sample from this population. The usual assumption which is made concerning the random errors is that they are distributed according to the Gauss or "normal" law of error. This law appears to be qualitatively correct since repeated observations of a single quantity support the idea of a continuous distribution with a single maximum and a montonic falling off toward zero on either side. In addition, such curves generally appear to be symmetrical. In practice, the number of measurements of a given quantity may be quite small and the available data may or may not be distributed in a manner approximating the normal law. This situation prevailed in this investigation. Only a single measurement could be performed before the fluctuating motions inside a cloud would change the experimental conditions. Thus we lacked information either to confirm or reject the assumption that the semi-objective estimates of the radar parameters and the cloud parameters would be distributed normally if a sufficient number of measurements could be performed. However, since repeated measurements of many physical quantities are distributed normally, we decided to make the assumption that the measured values and estimates of these parameters were random samples from a population which satisfied the normal law of error. This assumption allowed us to be more exact in the specification of the limits of error since we could employ the statistics of a normally-distributed variable.

When observational data are distributed normally two measures of dispersion that are in common use are the standard deviation (S.D.) and the probable error (P.E.). If $\bar{M}$ represents a particular value of the liquid-water content which has been measured by the radar, then the interval $\bar{M} \pm$ S.D. will cover the most probable value of M in 68.3% of the cases, in the long run. Similarly, the interval $\bar{M} \pm$ P.E. will contain the most probable value of M in 50.0% of the cases. If as we have assumed, the population of random errors is normally distributed, then

$$P.E. = 0.674 \text{ S.D.}$$

Griffiths [1967] has stated his experience led him to conclude that such semi-objective estimates of errors, when made by competent observors, are probably the limits that will not be exceeded nine times out of ten. If we assume that the absolute errors (designated by s) which have been computed in this chapter are the 0.90 confidence limits, then the most probable value of the variable of interest (say M) will be found in the interval $\bar{M} \pm s$ in 90% of the cases. Again, if the population of random errors is normally distributed, then

$$s = 1.645 \text{ S.D.}$$

Based on the Griffiths' conclusion, it seemed reasonable to stipulate that the experimental errors of both the component and compounded terms were the limits which would not be exceeded nine times out of ten, in the long run.

Summary of Error Analysis

The error of the experimental results was analyzed by components. Semi-objective estimates of the component quantities were made by competent observers. It was assumed that these estimates corresponded to error limits that would not be exceeded in nine observations out of ten. Standard methods were used to compound these estimated components of error. The computed errors were rather large and indicated that subsequent measurements with the TAM-1 radar should be preceded by careful analyses of both the experimental design and the apparatus to determine possible reductions of these uncertainties.

CHAPTER V

CASE STUDY

The methods described in Chapter III were combined with the theory of Chapter II to determine point values of the liquid-water content and vertical speeds in several cumulus congestus clouds that formed in the vicinity of College Station, Texas, during July 1967. A knowledge of the liquid-water content at any given time leads to an estimation of the rate of transfer of water from the sub-concentration m to the sub-concentration M because of the coalescence process. The measured values of M were used to construct scalar fields with height and time as independent variables. From the scalar fields of M, values of gradients were determined for inclusion in the continuity equation. Values of the vertical speed for the point in the cloud where M was measured were computed from the continuity equation. The analyzed values of the vertical speeds were expected to give some indication of the validity of the error analysis of the continuity equation.

Locale of Study

The geographical area of this study surrounds College Station, Texas. This area lies approximately 75 to 175 mi inland from the Gulf of Mexico and covers a part of the Gulf Coastal Plain of Texas. The topography varies from the level coastal prairies in

the southeastern portions to gently undulating hills in the northwestern portions. Elevation varies from 200 to 600 ft.

The mean annual precipitation varies from 40 in. in the southeastern part of the area to 35 in. in the northestern portion. Frontal activity is at a minimum during the summer and most of the rain produced during this period is provided by cumuliform clouds. An occasional hurricane during the summer and fall months may produce copious amounts of rainfall.

Maritime air flowing off the Gulf of Mexico is the dominant feature of the climate of the area during late spring and early summer. In a 1958-59 investigation of convective precipitation in this same area, Clark [1960] reported an average of 45 to 50 days per year having thunderstorm activity. Maximum thunderstorm activity is observed generally during the midafternoon and early evening.

Collection of Primary Data

Radar data. The basic data used in the case study were obtained by the method described in Chapter III. Twenty-three separate clouds were studied. The number of echoes which were studied on different days is listed in Table 7.

The following information concerning any particular echo was recorded in tabular form as extracted from each photographic frame: time, azimuth angle, elevation angle, range and the gain-step which completely attenuated the echo.

Table 7. Basic data used in case study

Date	Time (CDT)	Number of Echoes Studied
7 July 1967	1343 - 1808	13
11 July 1967	1535 - 1756	7
12 July 1967	1425 - 1613	3

Thermodynamic data. Some knowledge of the thermodynamic state of a cloud was necessary before the coalescence transfer term and the atmospheric compressibility factor could be evaluated. Anderson [1960] has pointed out that the core of a cloud in the early stages of its development has a temperature lapse rate that approximates the moist adiabatic lapse rate. Thus, for very large clouds, mixing of cloud air with environmental air may be of little importance at the core of the cloud. Based on the assumption of negligible mixing at the core between the surrounding air and cloud air, the moist adiabatic lapse rate was used together with appropriate values of density and pressure to specify the thermodynamic state.

The temperature soundings used in this study represented averages of those made at 1900 CDT at Fort Worth and Victoria, Texas, and Lake Charles, Louisiana. Mean soundings for each of three days are given in Table 8. The mean height of the convective condensation level was approximately 5,000 ft. This height varied less than 500 ft on each of three days and for each individual

Table 8. Thermodynamic data used in case study

	7 July 1967			11 July 1967			12 July 1967		
	θ_w = 23.5°C			θ_w = 24°C			θ_w = 23°C		
H	P	T_A	T_c	P	T_A	T_c	P	T_A	T_c
10^3ft	mb	°C	°C	mb	°C	°C	mb	°C	°C
2	942	25	25	942	23	23	942	23	23
4	882	20	20	883	19	21	883	19	19
6	821	18	18	822	16	18	822	15	16
8	763	13	14	765	11	15	764	9	13
10	712	8	11	710	8	12	710	6	10
12	660	5	8	661	4	9	658	4	7
14	612	1	4	613	1	6	610	0	4
16	572	-3	1	571	-3	3	568	-4	0
18	528	-6	-3	530	-7	-1	525	-7	-4
20	488	-12	-7	492	-11	-4	486	-12	-7
22	453	-17	-10	452	-15	-8	448	-16	-11

H = height above mean sea level

P = pressure

T_A = ambient air temperature

T_c = in-cloud temperature

sounding, thereby attesting to the homogeneity of the air mass. The wet-bulb potential temperature (θ_w) also was essentially the same for each of the three days. The slight day-to-day variation in θ_w indicated that the clouds which formed on the three days had similar meteorological properties. This latter characteristic helped insure that the sampling was from a population that was reasonably homogeneous.

Analysis of Primary Data

After the primary data were tabulated, some preliminary computations and analyses were made to determine values to be subtituted into Equation (56). In this section discussions are presented which summarize these computations.

Height of the radar beam. The height of the unit volumes of cloud that were delineated by the radar beam was assumed to be the height of the center of the beam. The values of the height of the center of the beam were calculated using an equation given by Bent et al. [1950], viz.,

$$z = 5280\ r \sin\omega + \frac{r^a}{2} + z_0 \ , \qquad (62)$$

where z is the height in feet above mean sea level, r is the range of the target in statute miles, ω is the elevation angle of the radar beam, and z_0 is the height of the radar antenna above mean sea level. The center of the parabolic reflector of the TAM-1 radar is 414 ft above mean sea level.

The vertical variation of the atmospheric index of refraction was computed for each of the three days of observation in order to determine the correction factor which should be applied to Equation (62) for non-standard propagation. The vertical gradient of the refractive index varied from standard conditions by a negligible amount. Therefore, standard propagation of the microwave signal was assumed.

Liquid-water content. Point values of liquid-water content were determined by insertion of values of $\bar{P}_r$ and r into Equation (47). To convert the gain setting of the receiver to a corresponding value of power received from a precipitating cloud, the following equation was used:

$$\bar{P}_r = 10^{P_d/10}, \tag{63}$$

where P_d is the average power received in dbm. The received power was measured at the receiver in decibels. The power in decibels was related to the gain-step decrements by the calibration technique described in Chapter III.

Since the values of M computed from Equation (47) probably are underestimations, the values of $\bar{P}_r$ were increased by 1.4 dbm to account for this systematic error. This correction was recommended by Probert-Jones [1962].

Scalar fields of M, with time and height as independent variables, were constructed from the measured values of liquid-water content. Figure 6 on page 80 shows the time-height cross

section for Echo 3, which is typical of the echoes that were studied. Values of $\Delta M/\Delta t$ and $\Delta M/\Delta z$ were measured using centered differences at various grid points of the time-height cross section. An increment of time of 8 min was chosen. This is approximately the time required to "examine" an echo from the lowest altitude (about 7000 ft) to the highest altitude (of the order of 22,000 ft). Only portions of the echoes which were at altitudes lower than 20,000 ft were studied in order to insure that only liquid drops were being illuminated. An increment of height equal to 4000 ft was chosen since this corresponds to the approximate width of the radar beam at the range of the echoes which were studied. Values of M were determined at these same grid points by interpolation.

A technique employed by Clark [1964] was used to evaluate $\Delta(M\bar{V})/\Delta z$. This technique consists of determining scalar fields of the momentum, $M\bar{V}$. Finite difference approximations are made in a manner similar to the method used in the estimation of $\Delta M/\Delta t$ and $\Delta M/\Delta z$. Point values of $M\bar{V}$ were determined from

$$M\bar{V} = \frac{\pi\rho_L N_0}{6}\int_0^\infty \exp(-ba)a^3\bar{V}da$$
$$= \pi\rho_L N_0 \bar{V} b^{-4}. \qquad (64)$$

The appropriate value of b^{-4} was determined from Equation (23). Solution of this equation for b gives

$$b = 22.4\ M^{-0.25}, \qquad (65)$$

where b is in units of cm^{-1} and M is in units of gm m^{-3}. Values of $\bar{V}$ depend on the diameter of the median-volume drop and the temperature and density of the ambient air. When a drop is falling at terminal velocity, the viscous, bouyant, and gravitational forces sum to zero. Such an equilibrium condition may be stated as

$$V^2 = \frac{4ga(\rho_L - \rho)}{3\rho C_D} , \qquad (66)$$

where g is the acceleration due to gravity and C_D is the coefficient of drag. The drag coefficient varies with the density and temperature of the ambient air as well as with the diameter of the drop. Clark [op.cit.] also outlined a procedure for computing C_D which leads to the determination of $\bar{V}$ from Equation (66). With ρ_L assumed to be 1 gm cm^{-3}, if C_D and ρ are known, then substitution of the diameter of the median-volume drop in Equation (66), together with these above-mentioned quantities, will give values of $\bar{V}$. In Chapter II we showed that the velocity of the drop having the median-volume diameter was essentially the same as the volume-mean velocity. This latter velocity was the one appearing in the continuity equation of M. Substitution for values of $\bar{V}$ and b in Equation (64) gave values of $M\bar{V}$ applicable to a point, and a finite-difference technique was used to determine $\Delta(M\bar{V})/\Delta z$.

Compressibility. As stated in Chapter II, effects of atmospheric compressibility were accounted for by the term $\Delta(\ln\rho)/\Delta z$.

To evaluate this term, the variation of ρ with height was computed. The density at a particular height can be related to the atmospheric pressure and temperature at this height by the equation of state

$$\rho = \frac{p}{R_d T^*} , \qquad (67)$$

where R_d is the specific gas constant of dry air and T^* is the virtual temperature. Values of pressure and virtual temperature corresponding to the appropriate wet-bulb potential temperature were determined from a thermodynamic diagram and substituted for the quantities on the right-hand side of Equation (67) to determine the air density at that level. The natural logarithm of the density for a particular level was calculated and plotted as a function of height above mean sea level. It was possible to draw a straight line which passed through or very close to points that were plotted. Clark [op.cit.] differentiated Equation (67) with respect to height and substituted appropriate values for the derivatives of the parameters on the right-hand side of this equation. His results indicated that the variation in $\ln\rho$ with height was nearly linear. Within the accuracy of the measuring apparatus, a constant value of $\Delta(\ln\rho)/\Delta z$ seems reasonable. The slope of the straight line had the value -1.08×10^{-4} m^{-1}.

Transfer of mass by coalescence. The rate at which mass is transfered per unit volume from the ensemble of small drops to the ensemble of large drops (those which can be detected with

the TAM-1 radar) was designated in Chapter II by τ and was shown to have the following form in the case of the M-P distribution:

$$\tau = \frac{N_0^2 \pi^2 \rho_L^2}{24} \int_{a_M}^{\infty} \alpha^2 \exp(-b\alpha) d\alpha \int_0^{a_M} E(\alpha, \beta) \beta^3 \exp(-b\beta) (V(\alpha) - V(\beta)) d\beta \tag{68}$$

$$+ \frac{N_0^2 \pi^2 \rho_L^2}{48} \int_0^{a_M} \alpha^2 \exp(-b\alpha) d\alpha \int_\gamma^{\alpha} E(\alpha, \beta) (\alpha^3 + \beta^3) \exp(-b\beta) (V(\alpha) - V(\beta) d\beta.$$

The evaluation of the integrals in Equation (68) depends greatly on the functional form of the collection efficiency, $E(\alpha, \beta)$.

We stated in Chapter II that the collection efficiency indicates the fraction of small drops, initially on a collision course with a large drop, that actually do collide and coalesce with the large drop. The collection efficiency is the product of a collision efficiency and a coalescence efficiency. The collision efficiency is often defined as the fraction of all water drops which, initially on a collision course with respect to other drops, actually do collide with the other drops. The coalescence efficiency is the fraction of all collisions between drops which result in actual merging of the two drops into a single larger drop. The collision efficiency of a pair of drops is determined by the trajectories of the drops while they are subjected to gravitational, aerodynamical, and electrical forces. The coalescence between two drops depends on the electrical forces present, the chemical composition of the drops, the impact velocity of the drops, and the realtive humidity of the ambient air

[Semonin, 1967].

The values of E that are reported in the literature are the result of both empirical and theoretical studies. Reviews of both of these approaches and the results obtained are found in the texts of Fletcher [1962] and Byers [1965]. The majority of the investigations indicate that most cloud drops are of sufficient size and composition to produce a coalescence each time a collision occurs between two drops. The early studies of the collision efficiency between two drops were confined generally to studies of the viscous and gravitational forces acting on the trajectories of the drops. Electrical effects were often unknown or uncontrolled in the case of the experimental studies or were omitted from the theoretical investigations. Semonin [op.cit.] has recently published results of collision studies which include the effect of the electrical field. This paper also reviews much of the recent work of other investigators who have considered the effect of electrical forces on the collision efficiency.

If we consider only uncharged drops, calculations and experiments indicate that the collision efficiency is low if both of the drops involved are less than about 18μ in radius [Fletcher, op.cit.]. For drops of drizzle size (radius up to 50μ) the collision efficiency increases with increasing drop size. When the radii of the collecting drops are greater than about 50μ the collision efficiencies generally decrease to or remain fixed at constant values. For small drops of 10μ radius the collision efficiency

changes little as the collecting drop varies in size from that of drizzle drops to large raindrops with radii of approximately 3 mm. Throughout this range the collision efficiency varies from about 0.8 to 0.9 [Byers, op.cit.]. When the collected drops are of radii 15μ and 20μ the collision efficiency is very nearly unity.

For the purpose of investigations into the process of rain formation in cumulus congestus clouds, the electrical fields within these clouds must be considered. When raindrops begin to grow, the strength of the electrical field increases by an order of magnitude over the value measured during fair weather. Since water is a dielectric, a strong electrical field will induce dipoles upon the droplets that, in general, will be attractive and, as a consequence, increase the probability of a collision. In addition, if the drops bear net positive or negative charges the collision efficiency will be increased or decreased depending on whether the drops involved in a collision bear unlike or like charges. The results of various experimental and theoretical studies cannot be unified at present [Fletcher, op.cit., Byers, op.cit.]. These studies do indicate, however, some general effects of electrical fields on the collection efficiency. In the case of charges and field strengths comparable to those existing in cumulus clouds, the studies showed that the collection efficiency of large drops was altered very slightly, but a considerable enhancement of the coalescence process was noted

for small drops.

The foregoing descriptions of the variation of the collection efficiency had to be written in a functional form before Equation (68) could be evaluated. The results which were cited above indicated that a collection efficiency of unity seemed to be applicable to the coalescence process when the collecting drops were of the sizes to be found in echo-producing clouds. Consideration of the effect of electrical fields indicated that the collection efficiency of the large drops would be changed very slightly when these fields were accounted for, but the collection efficiency of the smaller drops was increased if the effect of the fields was considered. Thus, the effect of the electrical fields is to narrow the range of the magnitude of the collection efficiency over the drop sizes which are likely to be found in clouds that produce echoes. The choice of unity for E seems to be a reasonable one in light of the data that are currently available. Values of $E = 1.0$ were used in some recent theoretical studies [Telford, 1955, Kessler, 1963] and the results obtained were quite realistic. The study by Kessler showed how the time at which rainfall first reached the ground varied with different values of E. As E ranged from almost 0 to 1.0, the time of the commencement of surface rainfall increased by only 5 sec.

The assumption of unit collection efficiency greatly simplifies the integrands in Equation (68). The expressions used to represent $V(\alpha)$ and $V(\beta)$ were suggested by Clark [op.cit.]. In the first

integral $V(\alpha)$ was given by a polynomial of the fourth degree in α which was fitted to empirical data by a least-squares technique. This polynomial was very accurate for drop diameters greater than 100μ. The functional form for $V(\beta)$ in both of the integrals was taken to be the expression given by Equation (66) with β replacing a. At a particular height in a cloud it was necessary to evaluate the other quantities before the integration could be performed. Equation (66) is very accurate for drop diameters less than 100μ. For this reason the same expression was used as the functional form of $V(\alpha)$ in the second integral of Equation (68).

An exact evaluation of the two integrals was possible since the integrands consisted of products of elementary functions which could be separated into sums of elementary functions. Figure 4 shows values of τ as a function of the parameter b. The range of b that is shown in this figure corresponds to rainfall rates varying from drizzle ($b = 48\ cm^{-1}$) to heavy rain ($b = 15\ cm^{-1}$).

Point values of τ were calculated from Equation (68) by substitution of the value of b appropriate to the location. The measured values of M were converted to values of b by use of Equation (65). Values of τ as a function of height and time for Echo 3 are shown in Figure 5. These values are comparable to the average values of τ computed from the data given by Braham [1952] in a study of the mass and energy budgets of thunderstorms. For cells whose durations were similar to the ones studied in the present investigation, the average value

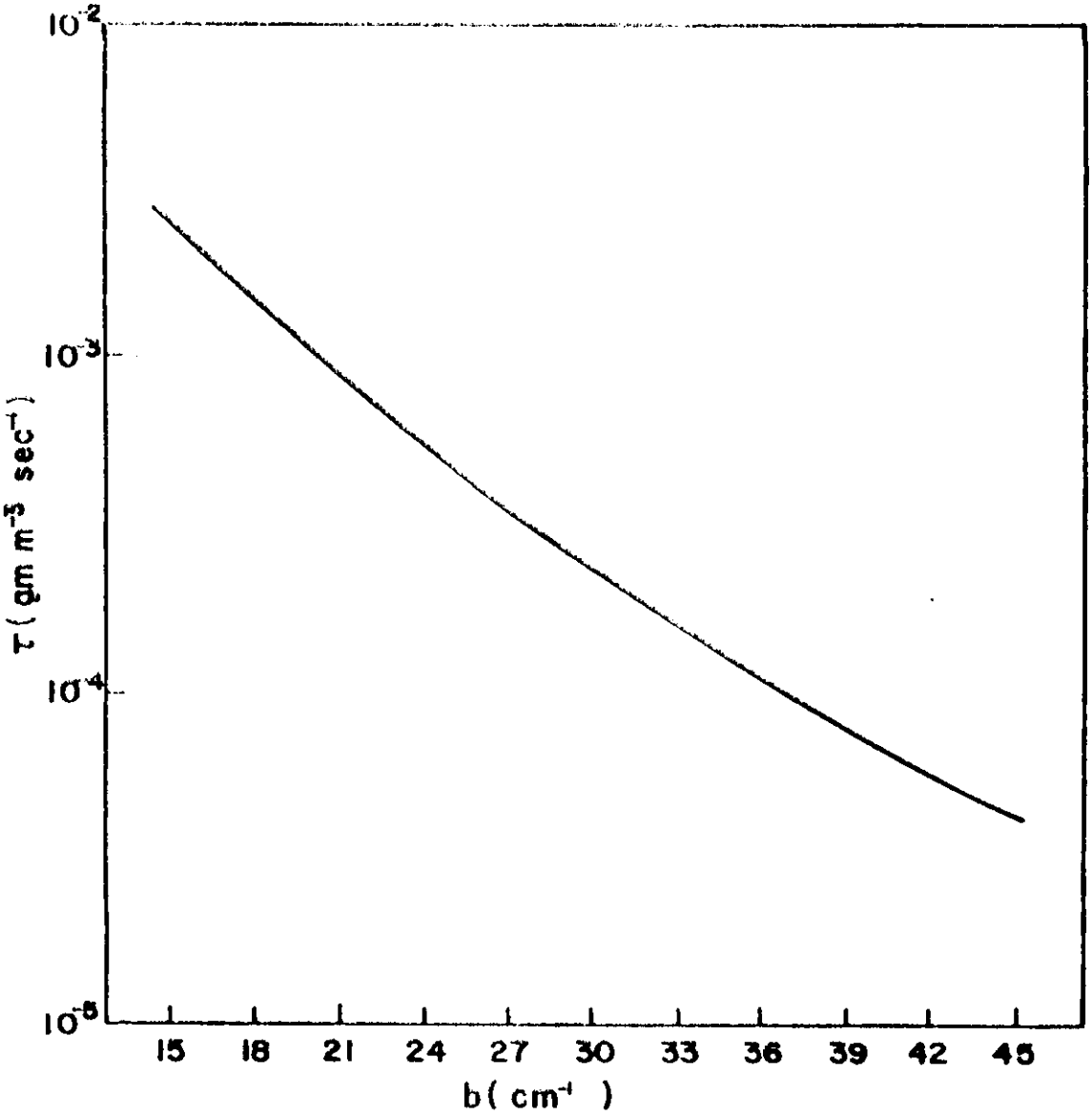

FIG. 4 THE VARIATION OF THE COALESCENCE – TRANSFER TERM WITH b.

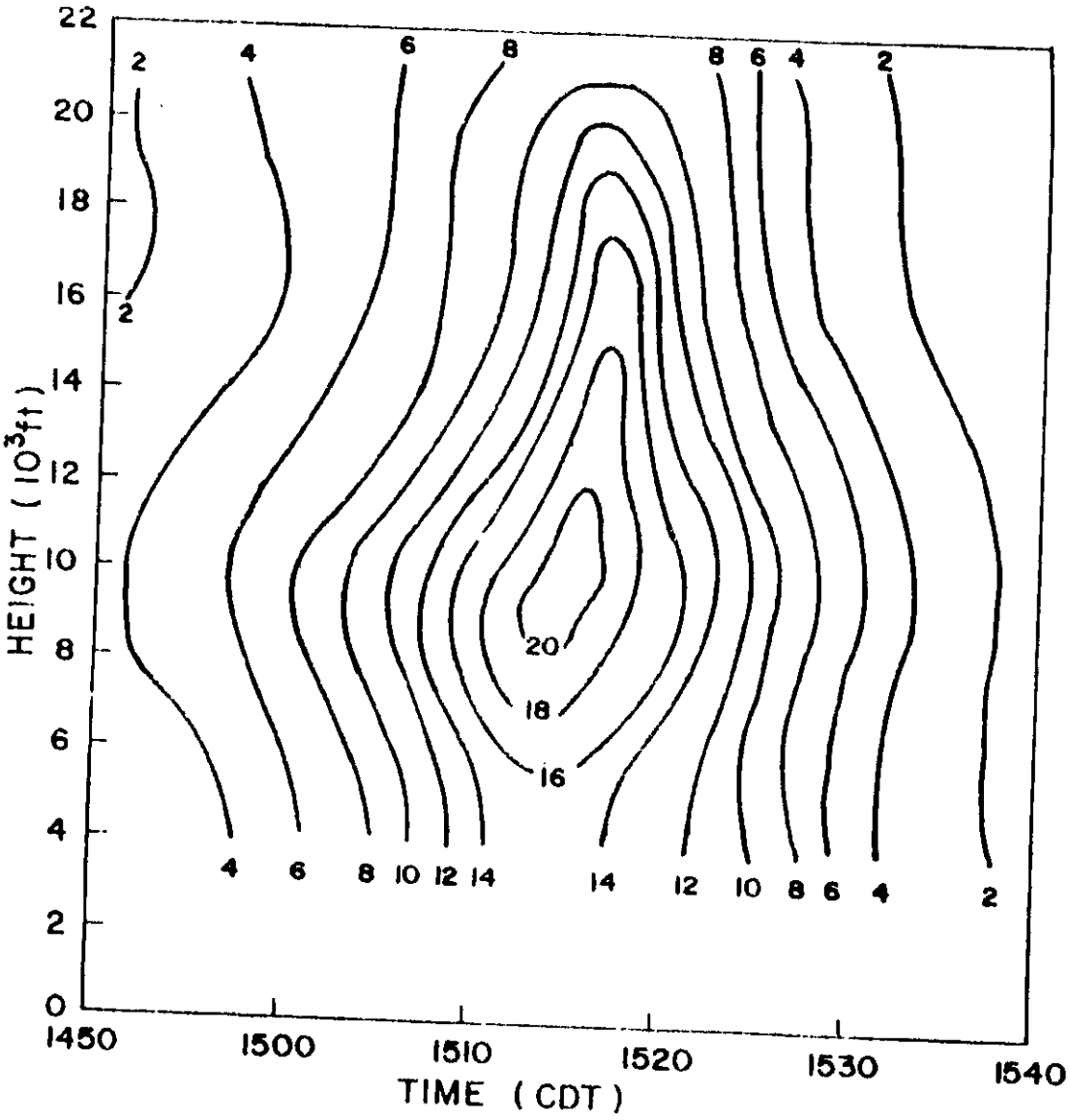

FIG. 5. TIME - HEIGHT CROSS SECTION OF THE COALESCENCE - TRANSFER TERM FOR THE CORE OF ECHO 3. ISOPLETHS OF T ARE IN UNITS OF 10^3 GM M^{-3} SEC^{-1}.

of τ was of the order of 10^{-3} gm m^{-3} sec^{-1}.

Results of the Case Study

The results of the analyses of each of the twenty-three echoes varied from echo to echo. However, it was possible to discern features which were common to the whole class of echoes. In this section the results of these analyses are presented.

Moisture field. The moisture field for Echo 3 is presented in Figure 6. The initial phases of the cycle were characterized by an increase of liquid water as the updrafts supplied vapor and condensed water. As soon as the drops were of sufficient size to produce a radar echo, a downward extension of the echo was noted. This extension was interpreted to be the result of the drag-induced downdraft and the coalescence mechanism which produced radar-detectable drops as coalescences occurred. The base of this cloud was estimated to be 5000 ft MSL, which was the convective condensation level.

Figure 6 is typical of the time-height cross sections which were constructed for each of the other echoes studied during this investigation. Each pattern was essentially symmetrical with time, indicating a cyclical increase of moisture that was followed by a decrease as the cloud passed to the dissipating stage. Another characteristic of each echo was the increase of liquid water with height until a maximum was attained. Bowen [1951] showed that such a maximum was expected in the region of the

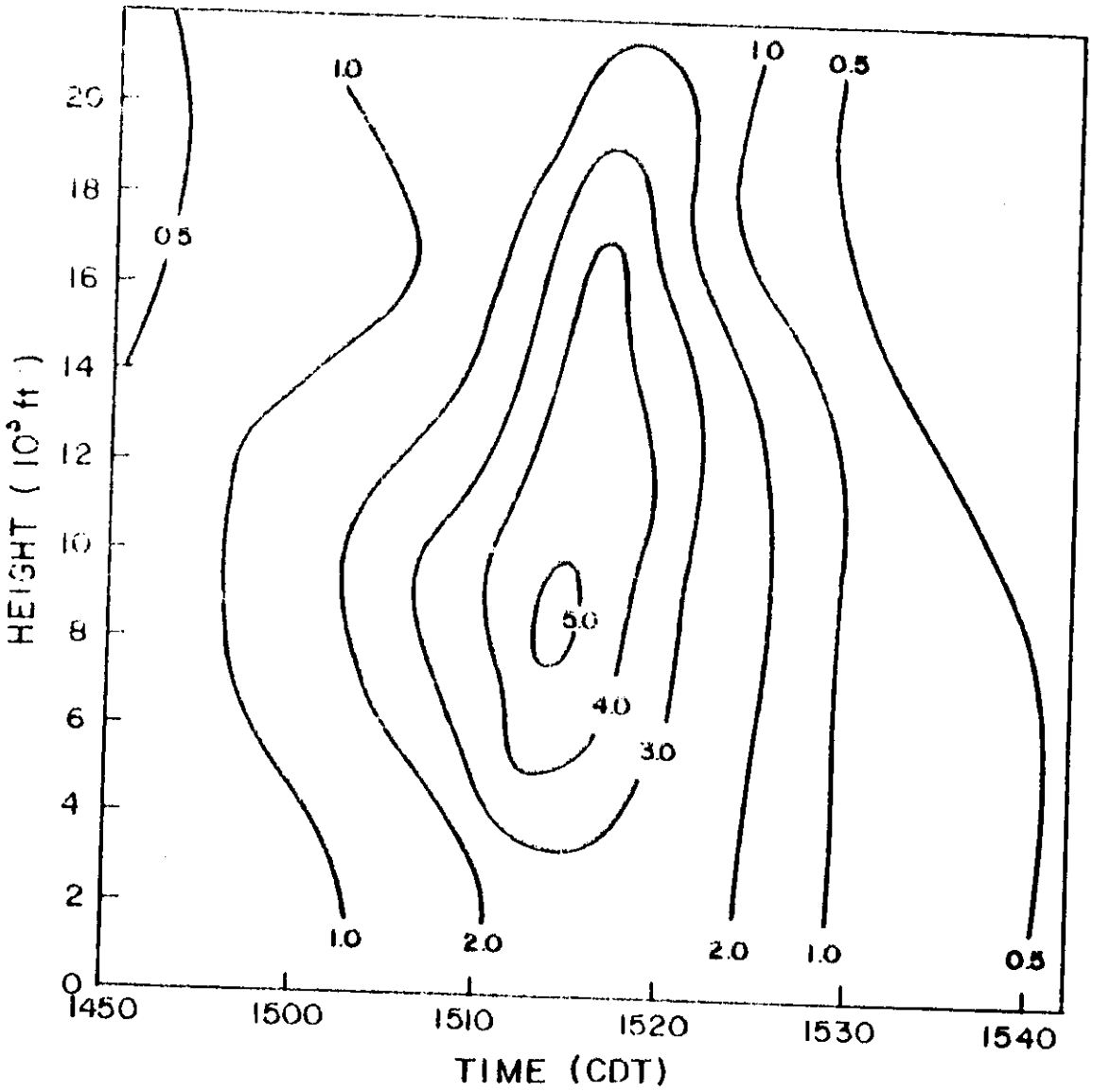

FIG. 6 TIME-HEIGHT CROSS SECTION OF LIQUID-WATER CONCENTRATION FOR THE CORE OF ECHO 3. ISOPLETHS OF LIQUID-WATER CONCENTRATION ARE IN GM M^{-3}.

cloud where $\bar{V} - w = 0$ if the coalescence process were the mode of rain formation.

In spite of the large error of M that was estimated in Chapter IV, we felt that the form of Figure 6 was qualitatively correct since the pattern is reasonable for a convective cell undergoing cyclic development. The point measurements of M that were used to construct this cross section may have fractional errors as large as 102.4% at the 0.90 level of confidence. The construction of scalar fields from these point measurements introduced a smoothing which produced a field that was qualitatively reasonable. Reduction of the experimental error would produce a pattern that would have a similar shape but the reliability of such a pattern would be much higher.

Some of the values of liquid-water concentration that are shown in Figure 6 are comparable to those reported by other investigators [Fletcher, op.cit. and Byers, op.cit.]. However, when all of the echoes were considered, some rather large values of liquid-water content appeared. The 695 point measurements from all of the echoes were grouped and the frequencies were plotted to show the variation of these data. Figure 7 shows the results of this grouping.

Measurements of liquid-water content that were made from instrumented aircraft generally showed that average values range from approximately 0.10 to 1.50 gm m^{-3} with mean values of the order of 0.50 gm m^{-3} [Ackerman, 1959, Fletcher, op.cit.].

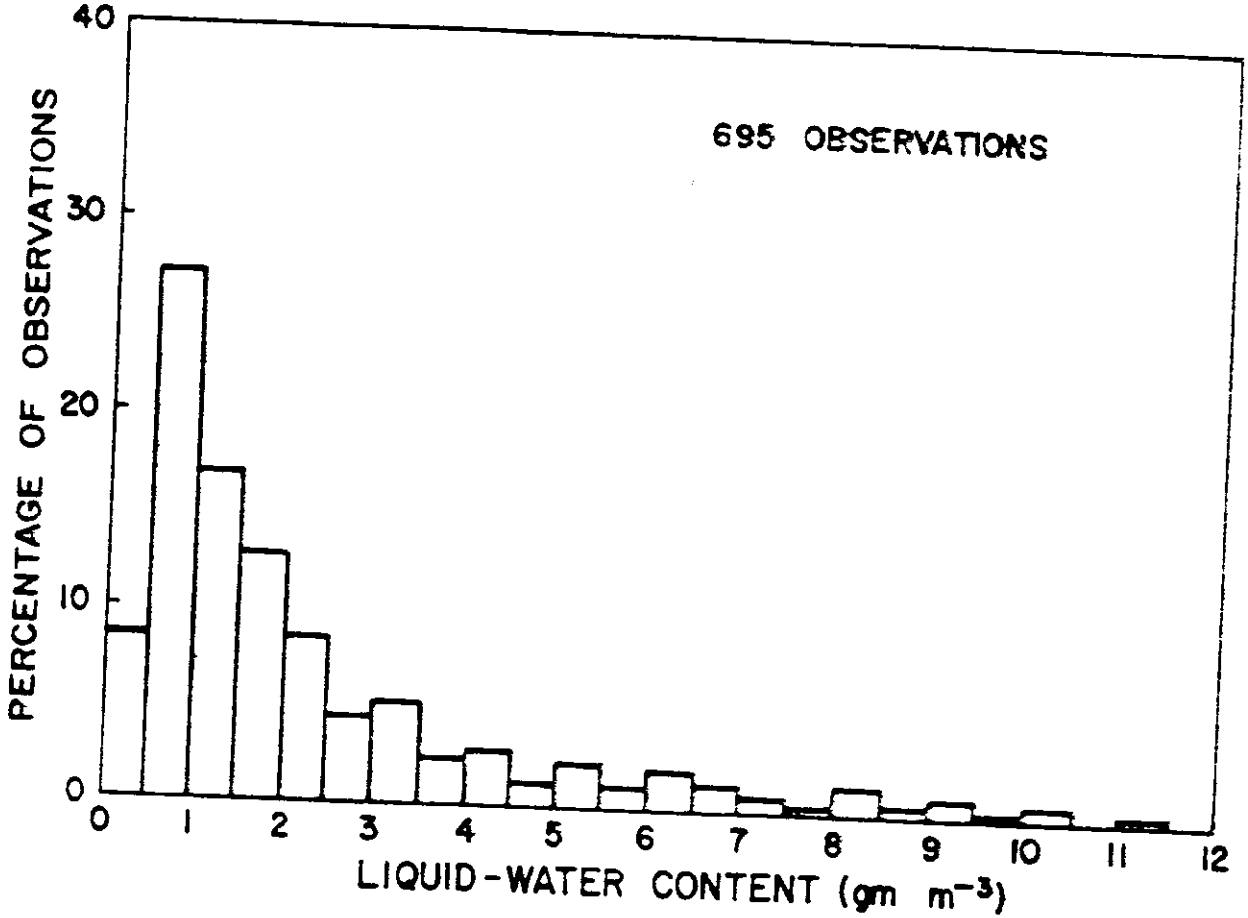

FIG. 7. HISTOGRAM OF THE PERCENTAGE OF OBSERVATIONS OF LIQUID-WATER CONCENTRATION THAT ARE CONTAINED IN THE CLASS INTERVALS INDICATED ON THE ABSCISSA.

These same sources report maximum values ranging from approximately 0.20 to 3.50 gm m^{-3} with means of about 1.50 gm m^{-3}. The mean of the data presented in Figure 7 is 2.17 gm m^{-3}.

Certainly, not all the individual measurements which comprise the data of Figure 7 can be interpreted as average values of liquid-water content. Some represent values corresponding to measurements made early and late in the cycle of the convective cell when values might be less than average and some of the measurements were made at times when maximum concentrations of liquid-water content were being observed. Thus, some caution must be exercised in comparing the values reported in the literature and the radar-measured values. However, the fact that the mean of all observations was 1.45 times the mean of the maxima as measured by aircraft and 4.34 times the mean of the averages as measured by aircraft would indicate that an experimental uncertainty which was of the order of 1.024 was vitiating the results.

Although it is desirable to obtain values of the liquid-water content whose magnitudes are physically reasonable, it is equally important that the spatial and temporal pattern of these measured quantities also be physically meaningful. Point values of M must be related to other values in the neighborhood of the point in question. With an experimental error as large as that estimated for the apparatus used in this study, both the magnitudes and the variations of these magnitudes with distance and time may be

atypical. We noted previously, however, that the fractional error of 1.024 did not seem to change appreciably the gross features of the fields of M.

The form of the moisture field associated with the core of Echo 3 is very similar to that of the idealized convective cloud described by Byers and Braham [1949]. They described the life cycle of a large convective cloud as consisting of three distinct stages of development. These are: a cumulus stage, characterized by updrafts throughout the cell; a mature stage, characterized by both updrafts and downdrafts, at least in the lower half of the cell; and a dissipating stage, characterized by weak downdrafts prevailing throughout the cell.

Figure 8 is a time-height cross section of the vertical speeds at the core of the idealized thunderstorm cell as presented by Byers and Braham [op.cit.]. This cross section is a useful one for comparison with the fields which were determined from the quantities measured by radar. The field of the vertical speeds at the core of Echo 3 is presented in the next section. The duration of the cumulus stage is depicted as the interval from the initial time to 13 min. During this stage, positive vertical speeds prevail throughout the convective cell and the first radar echo appears [Byers and Braham, op.cit.]. After the initial appearance of the radar echo, a rapid extension of the echo in the downward direction is often noted. This extension occurs at a rate that usually is greater than the fall speed

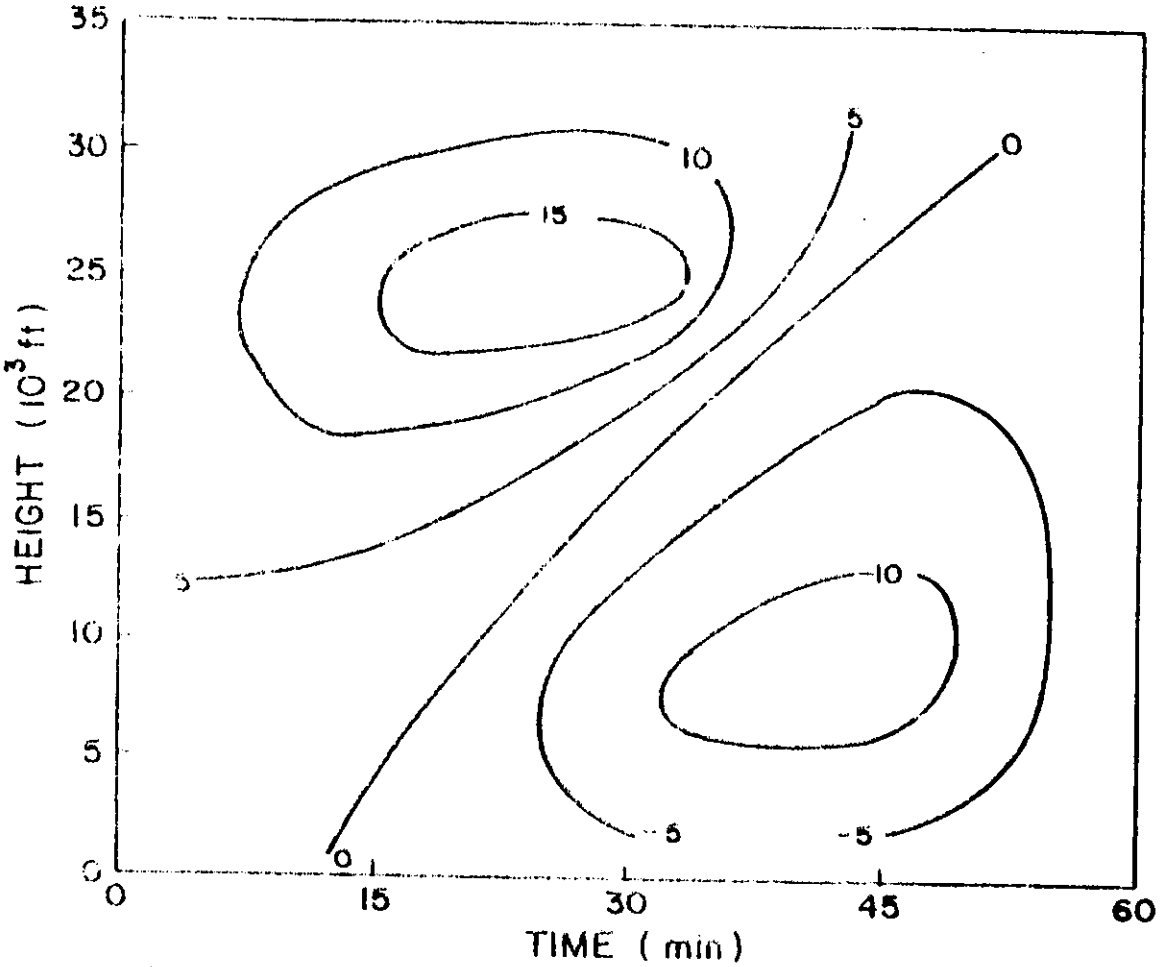

FIG. 5 TIME-HEIGHT CROSS SECTION OF THE VERTICAL SPEEDS FOR THE CORE OF AN IDEALIZED THUNDERSTORM ISOPLETHS OF VERTICAL SPEEDS ARE IN M SEC^{-1}

of the precipitation elements. This rapid growth of the echo suggests that the rain-producing mechanism is due to coalescence and that this mechanism proceeds at a very rapid rate.

The mature stage begins when rain falls out of the bottom of the cloud. Results of the Thunderstorm Project indicate that the initial appearance of the downdraft occurs almost simultaneously with the beginning of rain at the surface. In Figure 8 the mature stage is shown commencing after 17 min when the first negative speeds are detected at the ground. Downdrafts begin when the hydrometeors within a cloud have grown to a size that no longer can be supported by the existing updraft. As the larger hydrometeors fall relative to the ascending air they exert viscous drag on the rising air and the drag initiates a downdraft. As shown in Figure 8, the initiation of the downdraft first commences in the lower levels of the cloud where updraft speeds are smallest, since a smaller updraft speed has to be overcome by the descending precipitation. As time continues, the downdraft increases in vertical extent. Observations of the Thunderstorm Project indicate that the updraft continues to increase in speed with height during the mature stage, and the updraft also reaches a maximum early in this stage.

During the spread of negative vertical speeds, the convective cloud passes from the mature stage into the dissipating stage. This latter stage is characterized by downdrafts existing throughout the convective cell. A time of 45 min after initiation of the

cell may be selected as the beginning time of the dissipating stage of the idealized cell of Figure 8.

Field of vertical speeds. The time-height cross section of the vertical speeds at the core of Echo 3 is presented in Figure 9 and it contains some values that are quite unrealistic when compared to updrafts and downdrafts measured in such investigations as the Thunderstorm Project [Byers and Braham, op.cit.]. Time-height cross sections of vertical speeds were constructed for each of the 23 echoes which were studied. In many of these cross sections very large values of both positive and negative speeds were encountered. Each of the cross sections was similar to Figure 9, that is, the analyzed fields of vertical speeds contained values of vertical speeds that were reasonable, but the presence of unrealistic updrafts and/or downdrafts produced fields with little physical meaning or any systematic patterns comparable to the idealized cell of Byers and Braham. In order to achieve an over-all picture of these large updrafts and downdrafts, we decided to group the various vertical speeds. Percentage polygons of the updrafts computed from the continuity equation were constructed for altitudes of 5, 11, 16, and 20 thousand feet above mean sea level. Figures 10, 11, 12, and 13 show these polygons. These heights were selected to correspond to frequency distributions appearing in the report of the Thunderstorm Project. The percentage polygons representing the data from the Thunderstorm Project are shown as dashed lines

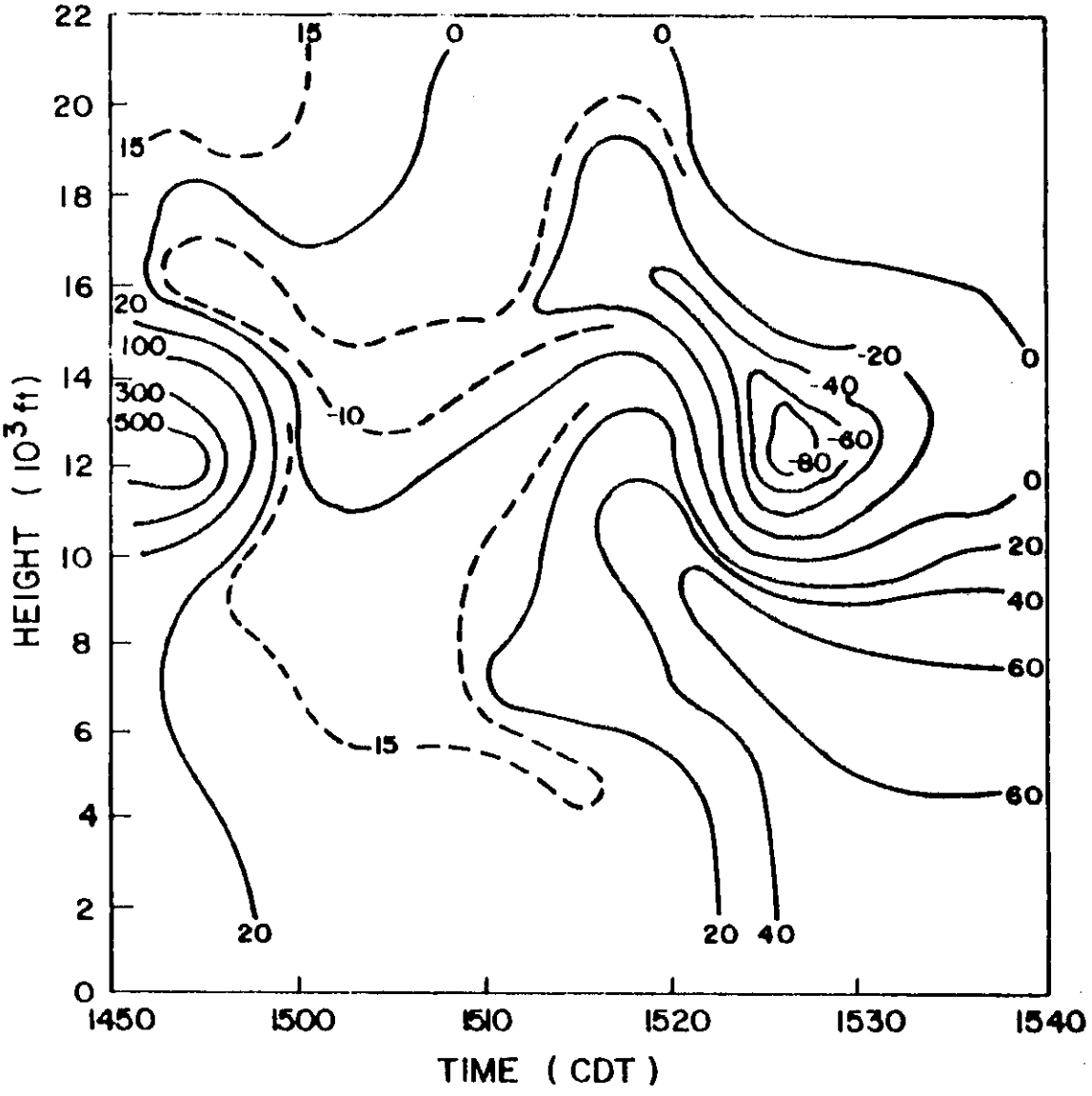

FIG 9 TIME-HEIGHT CROSS SECTION OF THE VERTICAL SPEEDS FOR THE CORE OF ECHO 3. ISOPLETHS OF VERTICAL SPEEDS ARE IN M SEC^{-1}.

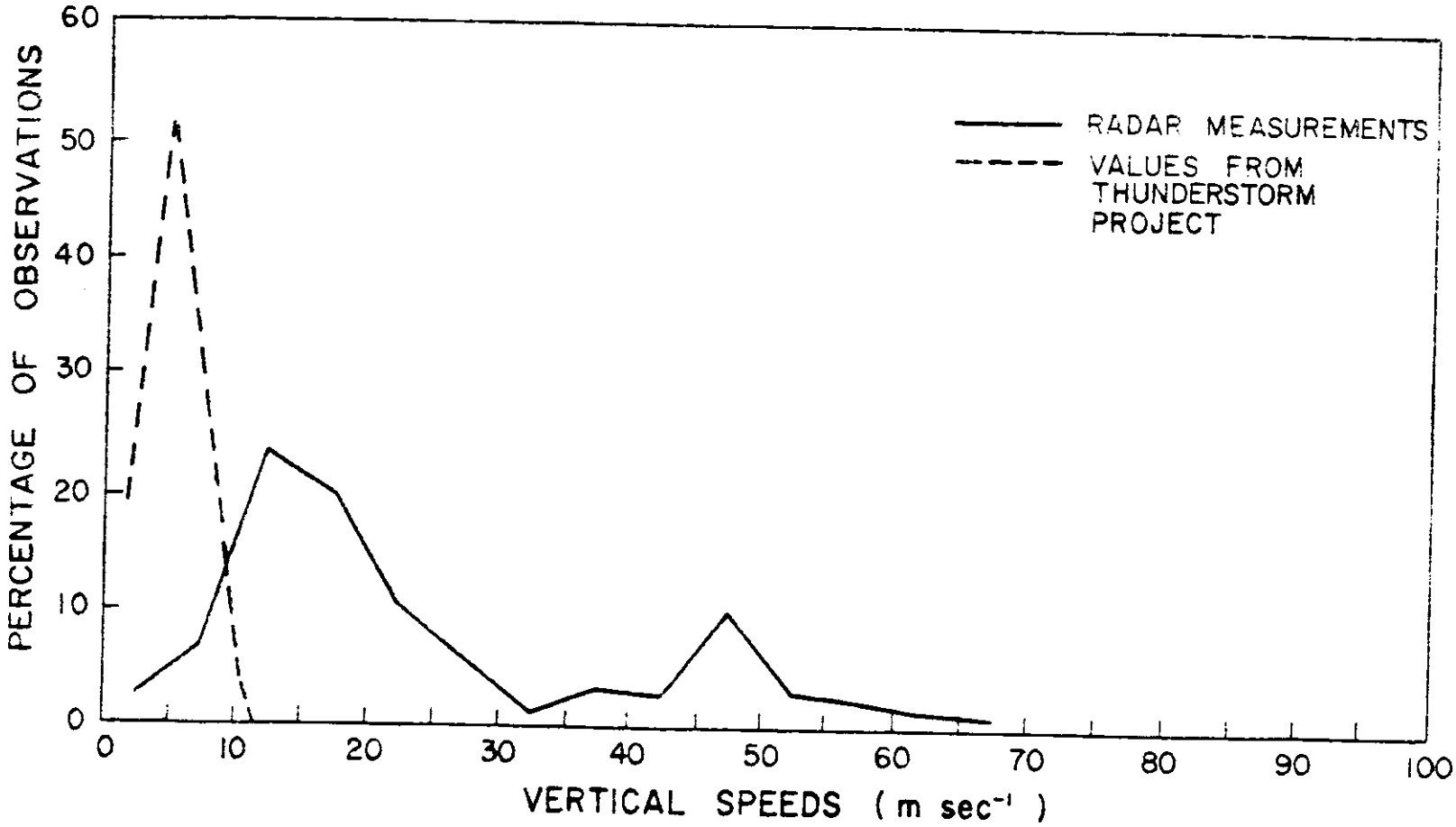

FIG. 10. PERCENTAGE OF OBSERVATIONS OF UPDRAFTS MEASURED AT 5,000 FT.

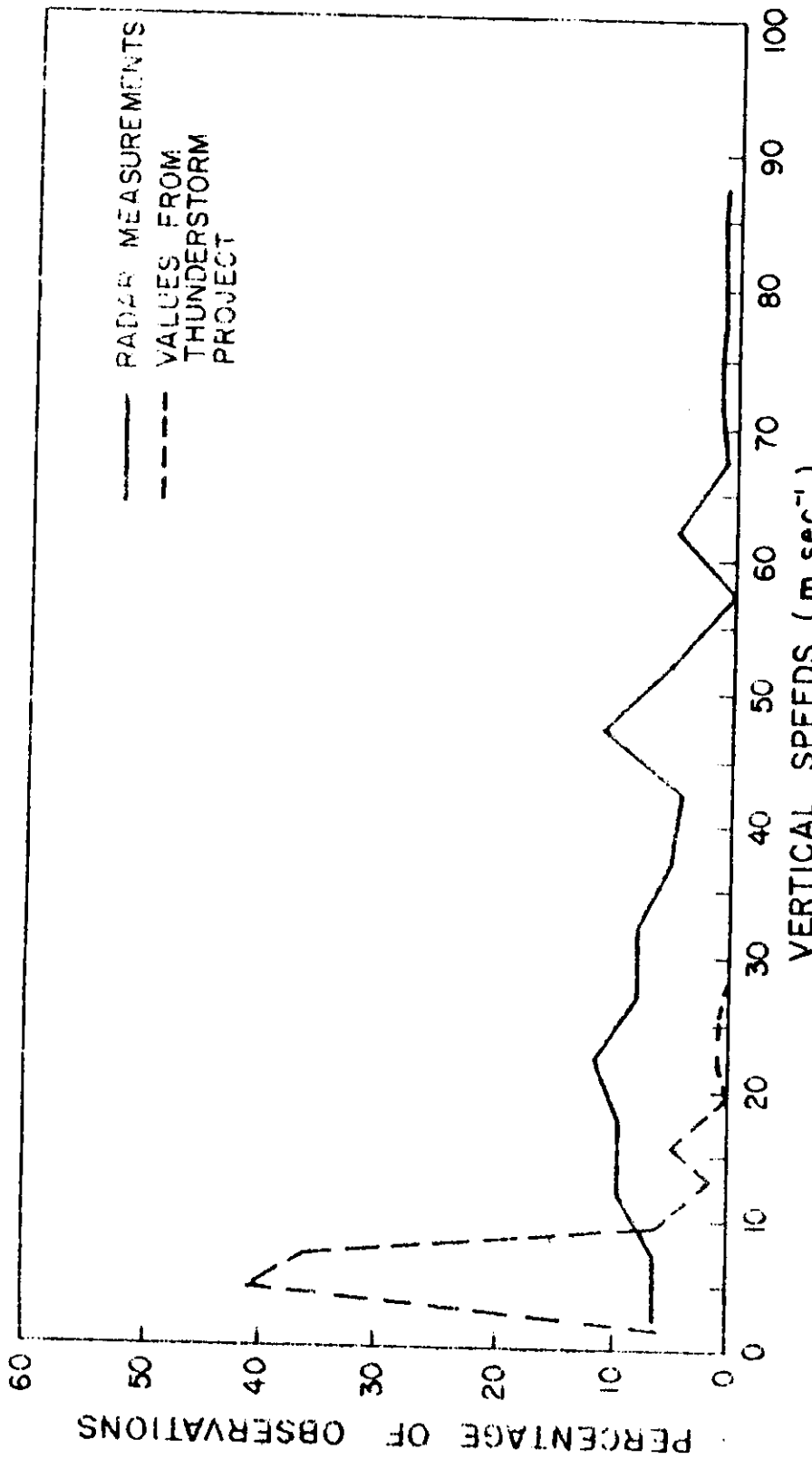

FIG. 11. PERCENTAGE OF OBSERVATION OF UPDRAFTS MEASURED AT 11,000 FT.

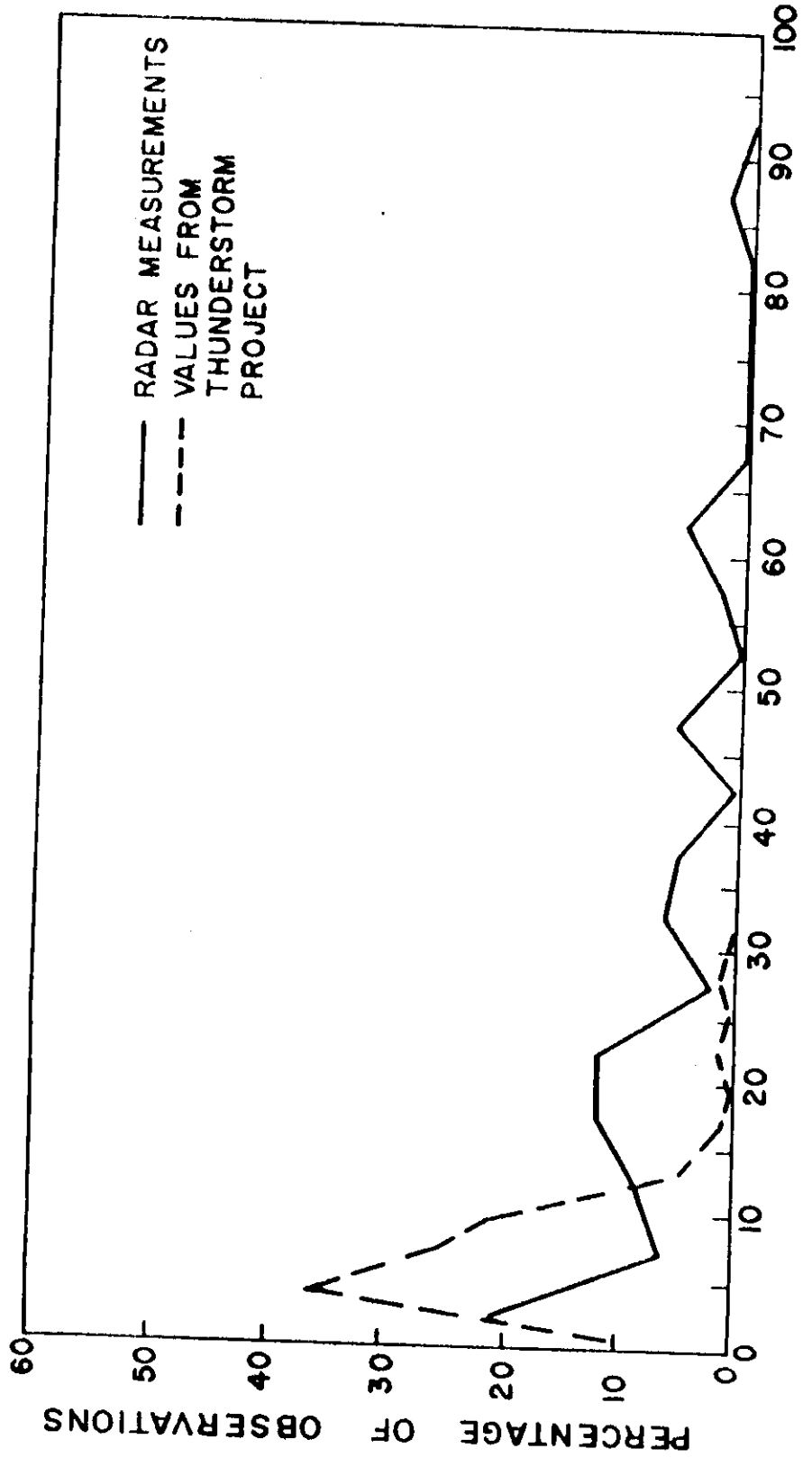

FIG. 12. PERCENTAGE OF OBSERVATION OF UPDRAFTS MEASURED AT 16,000 FT.

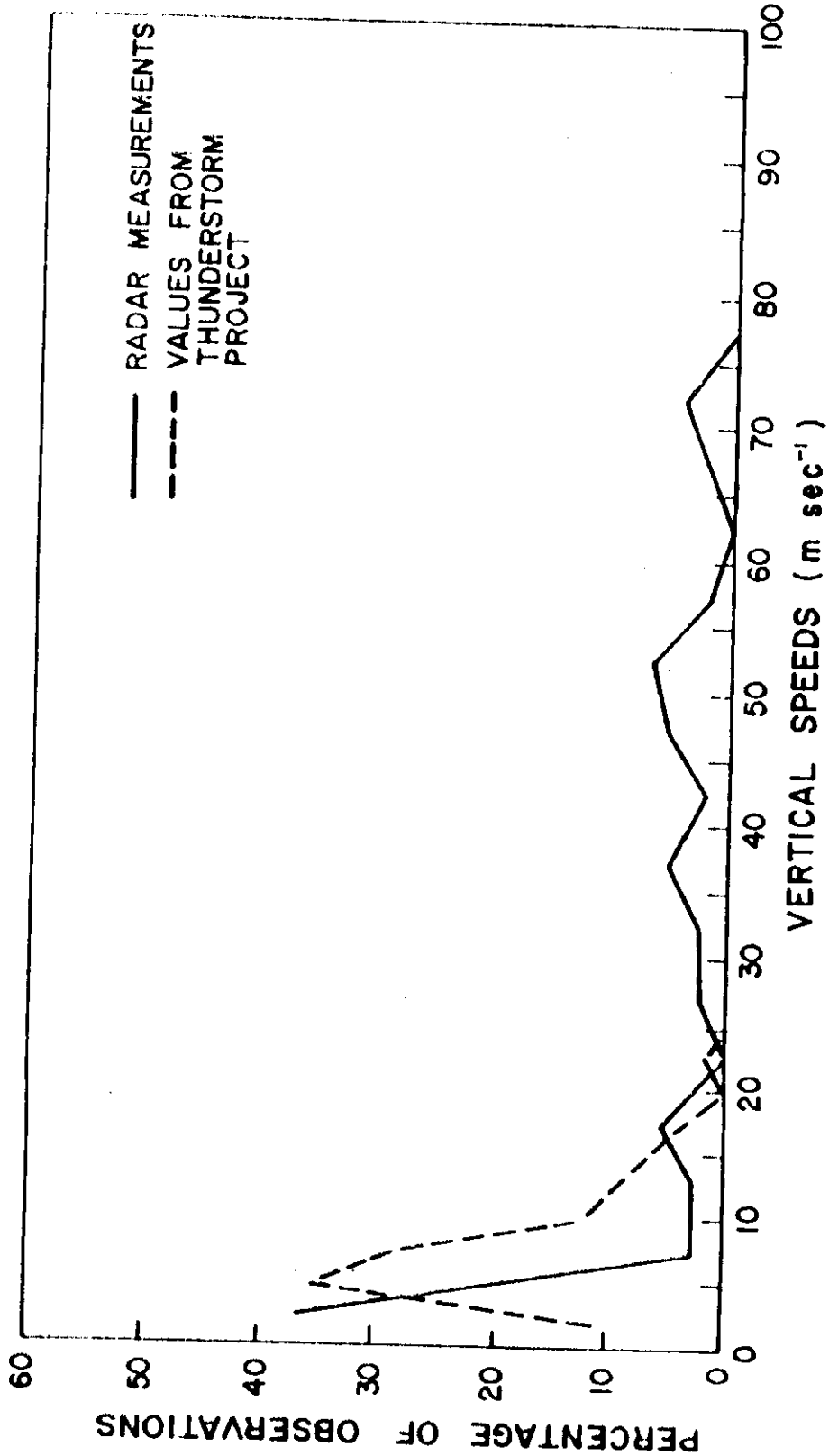

FIG. 13. PERCENTAGE OF OBSERVATION OF UPDRAFTS MEASURED AT 20,000 FT.

in the figures. Similar polygons were constructed for the downdrafts. These are shown in Figures 14, 15, 16, and 17. Several extreme values of vertical speeds were not shown in these figures because of the scale which was chosen. These extreme values are listed in Table 9.

Table 9. Extreme values of vertical speeds measured by radar

Altitude	Updrafts	Downdrafts
10^3 ft	m sec^{-1}	m sec^{-1}
4	104, 105, 143, 210, 212, 253, 510, 571, 895	374, 448, 569, 3674
12	123, 400, 553, 573, 838	110, 171, 189, 495, 632, 4325
16	103, 111, 882	153, 158, 448
20	104, 110, 148, 165, 208, 526, 1127	137, 336

When we considered the large error of w that was estimated in Chapter IV, it was easy to see how these extreme values could arise as well as the speeds whose values fell in the class intervals between 30 and 100 m sec^{-1}. In some instances the vertical speeds measured by radar that were less than, say, 25 m sec^{-1}

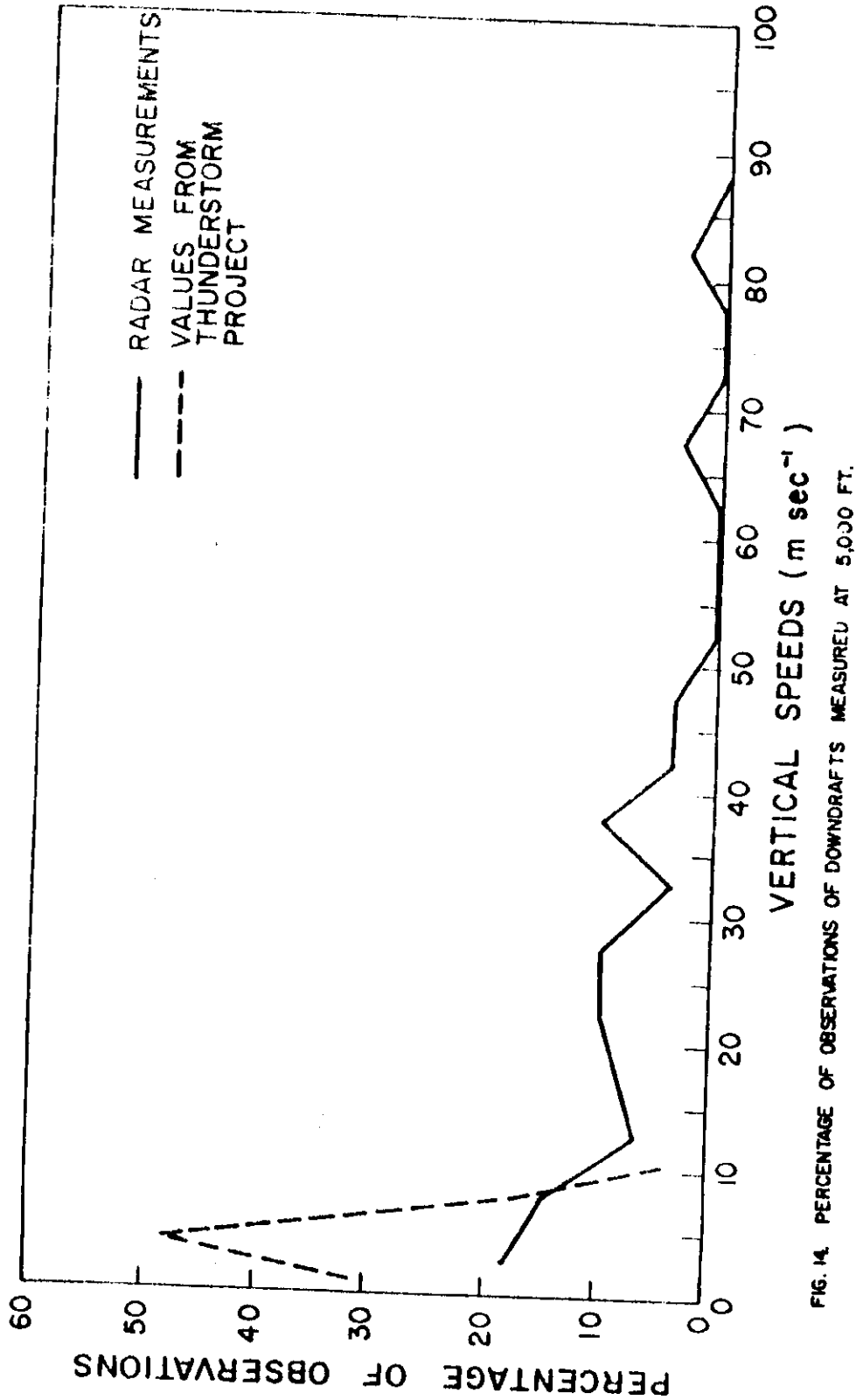

FIG. 14. PERCENTAGE OF OBSERVATIONS OF DOWNDRAFTS MEASURED AT 5,000 FT.

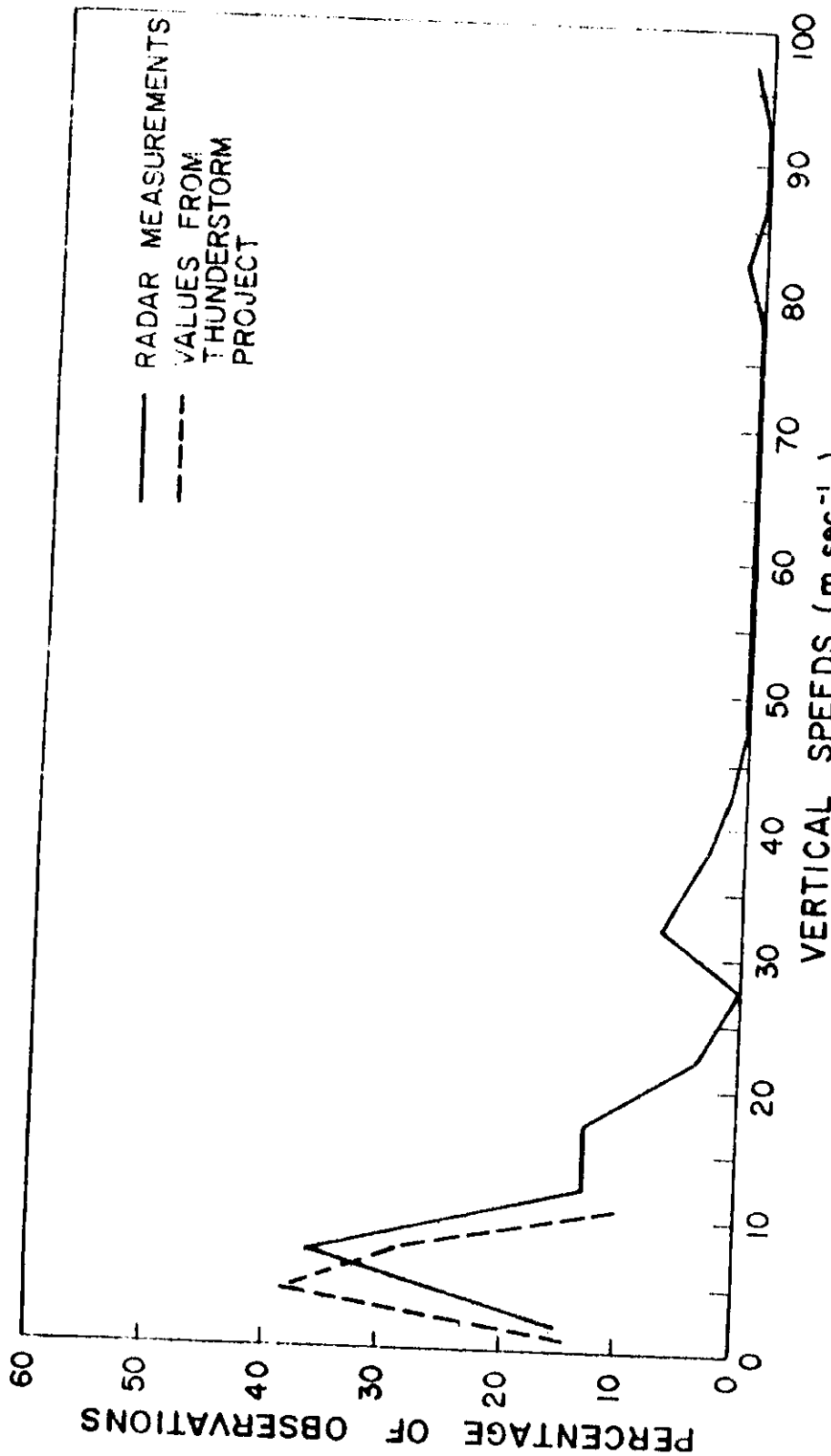

FIG. 15. PERCENTAGE OF OBSERVATIONS OF DOWNDRAFTS MEASURED AT 11,000 FT.

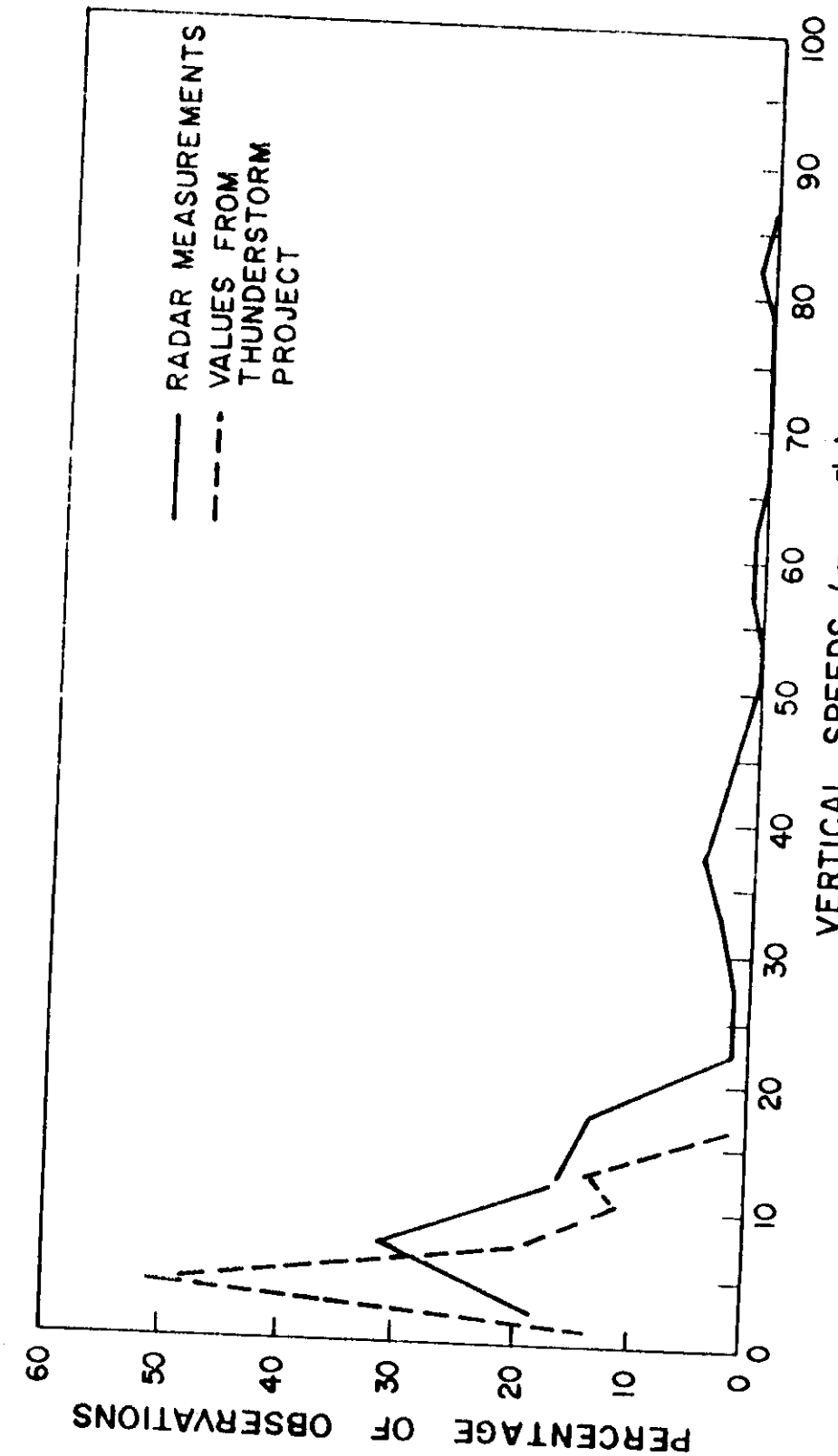

FIG. 16. PERCENTAGE OF OBSERVATIONS OF DOWNDRAFTS MEASURED AT 16,000 FT.

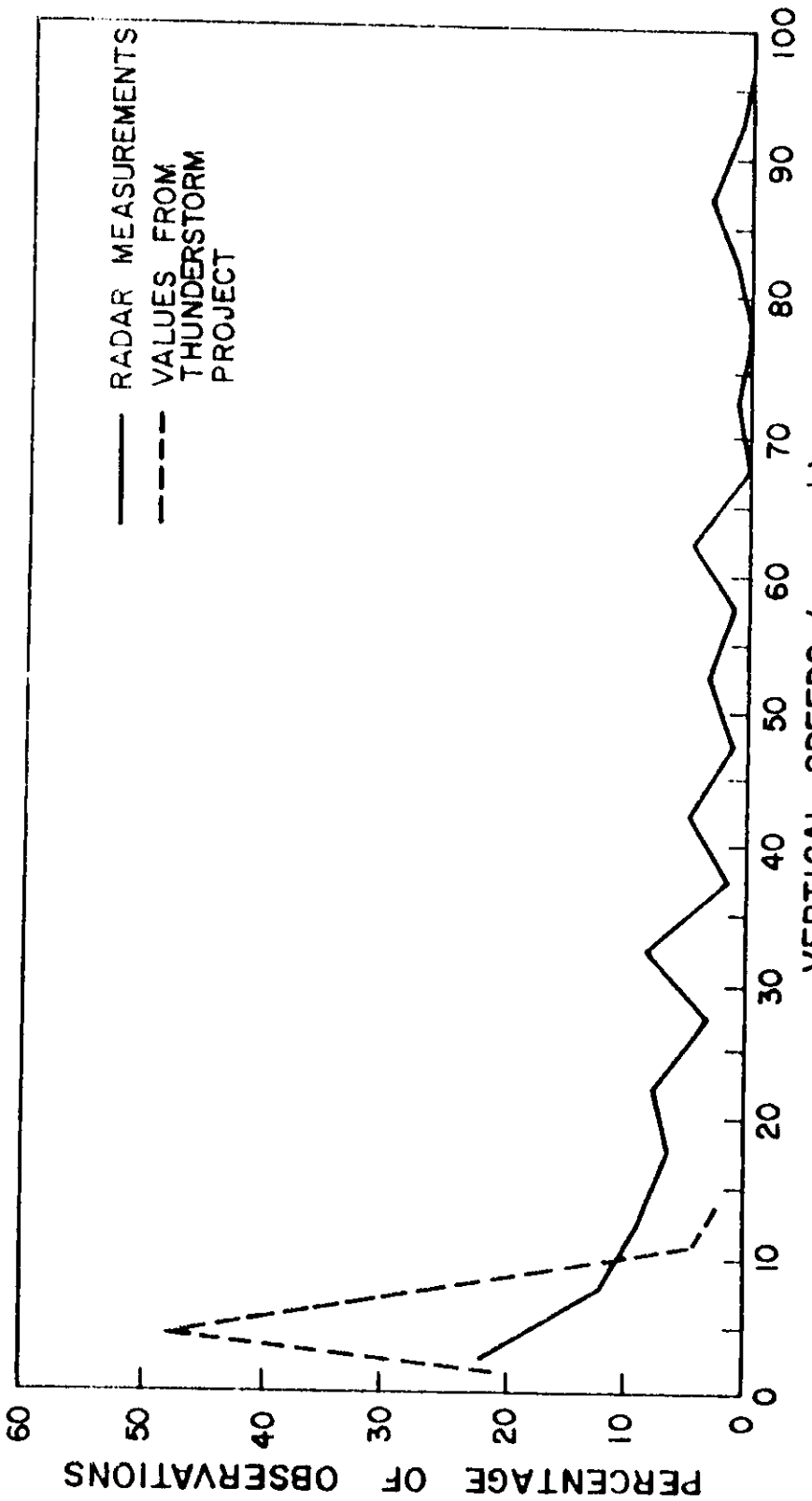

FIG. 17. PERCENTAGE OF OBSERVATIONS OF DOWNDRAFTS MEASURED AT 20,000 FT.

were in good agreement with the data from the Thunderstorm Project. The data which are summarized in Figures 12, 13, 15, and 16 agree reasonably well with the data from aircraft measurements. This agreement was not completely unsuspected since some of the radar-measured values of w, even with the large experimental error, were expected to agree with what may be termed "the more probable speeds" of the Thunderstorm Project. As in the case of the fields of liquid-water content, these large uncertainties in w have produced spatial and temporal patterns that are not typical.

Summary of the Case Study

Point values of liquid-water content were measured at the core of 23 convective clouds that formed near College Station, Texas. Scalar fields of liquid water were constructed for each cloud. The gross features of these fields appeared to be physically reasonable one, but the large experimental error inherent in the technique and apparatus caused certain point values in the field to be too large to be accepted. Gradients and time variations of liquid-water content were calculated from the scalar fields. These calculations together with a measure of the rate of growth of rain by coalescence were inserted into a continuity equation which then was solved for point values of vertical speeds. The experimental error was compounded in the computations of the vertical speeds with the result that time-height cross sections

of vertical speeds were quite unrealistic. Certain point calculations of vertical speeds were reasonable but many values were extremely large. Groupings of both the measurements of liquid-water content and vertical speeds indicated that the estimated magnitudes of the experimental errors were of the correct order.

C H A P T E R V I

REDUCTION OF THE MEASUREMENT ERRORS

Chapter IV dealt with the problem of calculating the errors of the computed quantities M and w in terms of the errors in the constituent quantities. In this chapter the converse problem will be considered, that is, how much reduction must be made in the errors of the constituent quantities in order to reduce the errors of M and w to some desirable level. The errors that contribute to the total error of w also appear in the computation of the error of M. Therefore, any reduction of the uncertainty of the measured values of M will produce a reduction in the errors of w.

Liquid-water Content

The fractional error of M is summarized in Table 4. The square of this error may be expressed as

$$S_M^2 = E_1 + E_2 + E_3 + E_4 \ , \qquad (69)$$

where the E's with subscripts 1 through 4 refer to the squares of the contributions to the fractional error of M by errors in the average received power, radar constant, range, and the dielectric factor, respectively. Substitution of the values recorded in Table 4 for the respective values in Equation (69) gives

$$S_M^2 = 0.3S_1^2 + 0.3S_2^2 + 0.3S_3^2 + 0,3S_4^2$$

$$= 0.692 + 0.349 + 0.008 + 0.000$$

$$= 1.049.$$

The subscripts of S correspond to the quantities mentioned previously. The numbers appearing in the middle row of this expression are the values designated by the symbols E_1 through E_4 in Equation (69).

The largest contributions to the fractional error of M were those of the received power and the radar constant. In a preliminary consideration of reducing the error of M, the effects of range and dielectric factor may be neglected. Since the contribution of the error of the received power is approximately twice that of the radar constant, a first step in the reduction of the experimental error is to consider decreasing the contribution of the received power until it is the same as the contribution of the radar constant. If the contribution represented by E_1 is reduced to 0.349, the corresponding fractional error of the received power becomes 1.080. In terms of power measurements in decibels this means that the received power would have to be measured with an accuracy of ± 3.2 dbm. After this reduction the error of M may be computed by substitution of the value 0.349 for E_1 in Equation (69). Solution of Equation (69) for S_M with this new value for E_1 gives $S_M = 0.838 = 83.8\%$. A fractional error of this magnitude is still quite large.

For further reduction of the error of M we may consider a

joint reduction of the errors of $\bar{P}_r$ and C_1 until their individual contributions to the total error are comparable to the contribution from uncertainties in the measurements of range. With both E_1 and E_2 assumed to have the value 0.008, as does E_3, the fractional error of S_M becomes

$$S_M^2 = 0.008 + 0.008 + 0.008$$
$$= 0.024,$$

and

$$S_M = 0.155 = 15.5\%.$$

A contribution of 0.008 to the total square of the fractional error of M, by the errors of $\bar{P}_r$, corresponds to an error of 16.3% or about 0.7 dbm. Thus, the averaged received power would have to be measured to within ± 0.7 dbm in order to insure that the measured values of M would be accurate to ± 16%. This error probably represents a lower limit since the value 0.008 represents approximately the minimum value that can be attained for the contribution to the total error from errors in measurements of range. This contribution (0.008) corresponds to an absolute error of ± 2 mi. This latter value represents the limits of the present equipment. The contribution by the range error represents an upper bound on the accuracy of the measurements of M. An error of 16% in the measured values of M is comparable to the accuracy of some aircraft instruments.

If the error of M is to be reduced to 16%, the question arises concerning the accuracy that is needed in the measure-

ment of the parameters that make up $\bar{P}_r$ and C_1. The accuracy in the measured values of both $\bar{P}_r$ and C_1 must be ± 16.3% if M is to be accurate to ± 16%.

We stated in a previous paragraph that an accuracy of ± 16.3% in $\bar{P}_r$ corresponds to approximately ± 0.7 dbm. Such accuracy may be difficult to attain with the present measuring and calibrating equipment. Both day-to-day variations in experimental conditions and the technique of calibration were estimated to introduce errors of 1 dbm in the measured values of $\bar{P}_r$. It would be desirable to reduce these by an order of magnitude. Such reductions might be achieved without modifying the present equipment if more precise calibrating instruments were used and if a careful check were maintained on the variations of the receiver response. The magnitudes which were estimated for the errors of the quantities comprising $\bar{P}_r$, as well as C_1, were not made with instruments but were the estimations of competent observers. Such semi-objective estimations probably contain components that can be designated as systematic errors once instruments are used. The systematic components can be accounted for by adjusting the measured quantities and the resultant random component will be much smaller.

The other factor contributing to the error of $\bar{P}_r$ was the size of the scale division that was used to record the magnitude of the received power. In this investigation a gain-step to 0.5 dbm would be necessary if each of the errors of the calibrations

and day-to-day variations can be reduced to 0.1 dbm. A reduction in the size of the gain-step, however, will require a longer time period to examine a complete echo from the lowest to the highest elevation. If the important features of the cloud are likely to change during such an expanded period of examination then some compromise must be achieved between the demands of more accurate power measurements and a reasonable time resolution. A receiver that contains an integrating circuit which averages the power contained in the pulses reflected from a precipitating cloud would help in the reduction of the error of $\bar{P}_r$. The error of measurement of such a receiver may be ± 10% [Huebner, 1967].

A reduction in the error of C_1 to ± 16.3% will require more precise measurements of at least four of the parameters that make up this term. Table 3 shows the relative contribution to the total error by the various constituent terms. It can be seen that improved measurements of the transmitted power, antenna gain, pulse length, and beam width are needed if the total error is to be reduced. In a previous paragraph it was stated that a fractional error of C_1 amounting to ± 16.3% was required if M is to be accurate to ± 16%. This amounts to a contribution of 0.008 to the total square of the fractional error of M. To achieve a contribution to the total error of 0.008, the square of the fractional error of C_1 must be reduced to 0.027. This is equivalent to the fractional error of 16.3%.

The desired reduction can be obtained by reducing the uncer-

tainty in the measurements of the gain and beam width by two orders of magnitude and reducing the uncertainty in the transmitted power by one order of magnitude. As in the case of the estimations of the errors of $\bar{P}_r$, some reduction in the uncertainties of P_t, G, and θ probably can be obtained by measuring these quantities with suitable instruments. In this manner, it is quite possible to convert some of the uncertainty to systematic errors which can be accounted for. The remaining random components will be much smaller. The uncertainties of P_t and G can be combined into a single value. Transmitted power is measured at a point in the wave guide between the transmitter and the focus of the parabolic reflector. Losses in the wave guide between this point of measurement and the reflector can be combined with the antenna gain to produce a somewhat smaller gain figure. With the term $P_t G^2$ in the radar constant considered as one parameter, repeated measurements of an unvarying target can be performed to determine possible systematic errors as well as the magnitude of the random errors. Reductions in the uncertainties of θ will require careful field measurements over a uniform test range. Austin and Geotis [1960] have outlined a technique for measuring many of the parameters in the radar constant. It would be worthwhile to consider their approach in future work using the TAM-1 radar. A straight-forward method employing a standard (unvarying) target in the calibration of a weather radar was discussed by Atlas and Mossop [1959] and the incorpor-

ation of this latter technique with that of Austin and Geotis offers a possible method for reducing some of the uncertainty in the measurements of the radar constant.

The actual reduction in the uncertainties of these constituent terms would require the use of calibrating instruments whose errors are known, as well as day-to-day checks on the radar equipment to insure that additional systematic errors were not affecting the measurements of M. In addition, any future investigation should include an experimental design that will account for possible extraneous effects and deviations from experimental control.

Vertical Speeds

Since the errors that contribute to the total error of M also appear in the computation of the error of w, it is possible to chart the reduction of the fractional error of w as more accuracy is attained in the measurements of M. Figure 18 shows the relationship between these two fractional errors. When the fractional error of w was computed in Chapter IV, values were used that produced very large estimates of the constituent errors. Perhaps such a large estimate was an overly cautious one. The grouped data, however, indicate that the 0.90-level error of w is quite large. The subjectivity in the evaluation of the errors of the M-field probably can be minimized by analyzing these errors in an objective manner. Research directed toward the analysis

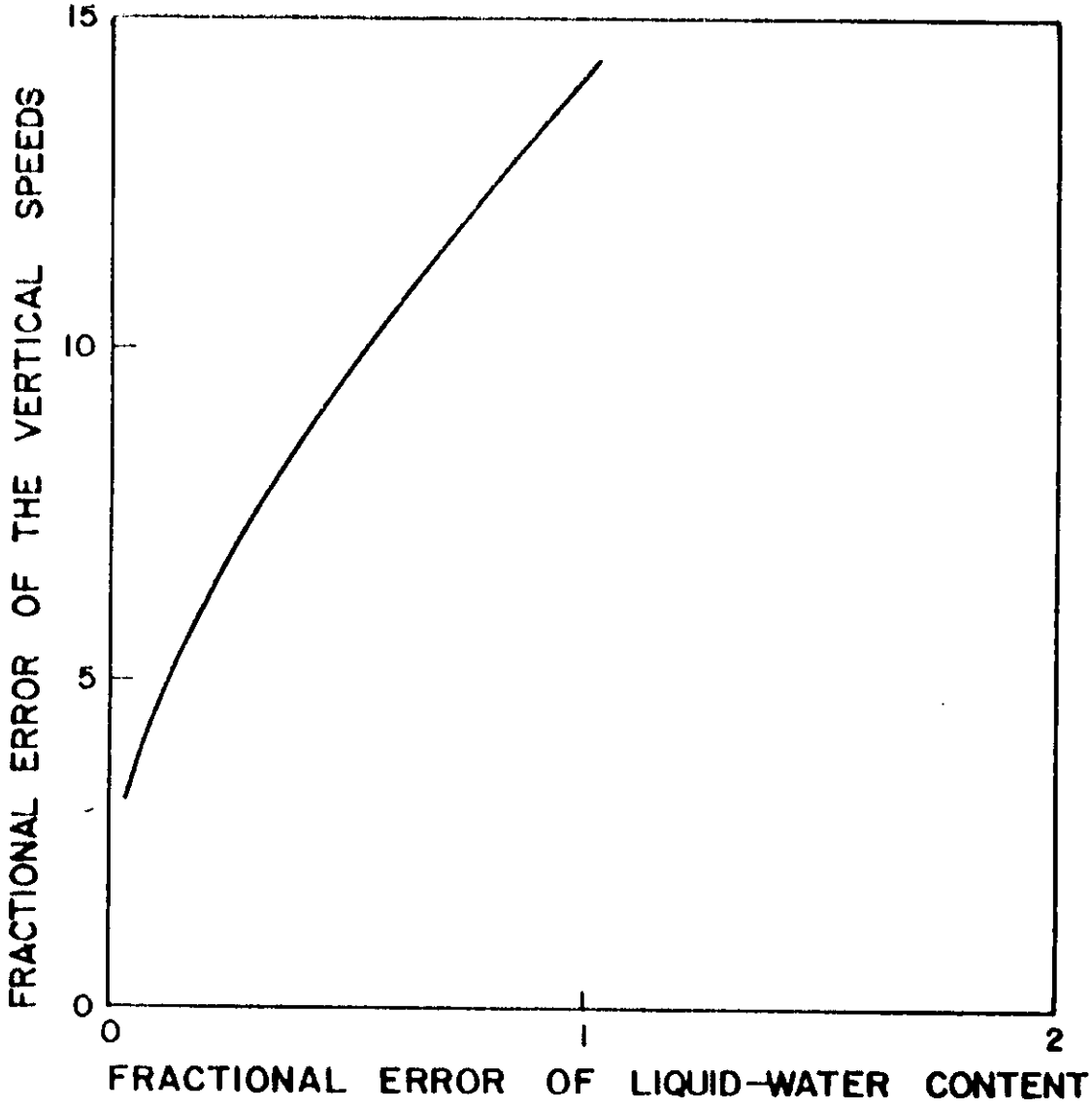

FIG. 18 VARIATION OF THE FRACTIONAL ERROR OF THE MEASUREMENTS OF VERTICAL SPEEDS WITH THE FRACTIONAL ERROR OF THE MEASUREMENTS OF THE LIQUID-WATER CONCENTRATION.

of the errors in scalar fields undoubtedly will produce immediate benefits.

Summary of Error Reductions

Any improvement in the reliability of the measurements of liquid-water content and vertical speeds will require a preliminary consideration of the systematic errors inherent in the measuring technique. The use of accurate instruments and controlled conditions should aid in the delineation of these systematic errors and provide a more reasonable estimate of the magnitudes of the random errors. At present, the TAM-1 radar is not operated with a degree of experimental control which assures such a delineation. Once the systematic errors are located, their effects can be removed by application of a suitable correction. The random errors which remain will be smaller than the original uncertainties and a higher degree of confidence can be placed on the magnitudes that are determined from the measurements. The preliminary calculations which were presented in this chapter indicate that the use of experimental control together with more accurate calibrating instruments may permit the measurement of liquid-water content with an accuracy of ± 16%. It does not appear that vertical speeds can be measured with more accuracy than ± 270%, even after the above-mentioned techniques are applied.

C H A P T E R V I I

SUMMARY AND RECOMMENDATIONS

Summary of Results

The results of this study indicate that reasonably accurate measurements of the liquid-water content in a cloud can be achieved with a radar operating at a wavelength of 10 cm if high experimental standards are maintained. The theoretical equation which relates the liquid-water content to the power received from a precipitating volume is expressed by Equation (47), viz.,

$$M = 3.94 \times 10^{-3}\left[\frac{\bar{P}_r r^2}{C_1 K^2}\right]^{0.56} . \qquad (47)$$

This equation has a systematic error that is small and can be accounted for if attenuation is negligible and the radar beam is completely filled. Use of the 10-cm wavelength assured the former while selection of convective echoes at ranges of less than 40 mi minimized the beam-filling error.

An error analysis of the experimental apparatus and technique was made. This indicated that the fractional error of measurements of liquid-water content is 1.024. It was surmised that a part of this error may be compensated for if careful measurements are made of the variables in Equation (47). Twenty-three echoes were studied and 695 measurements of liquid-water content were obtained from them. The grouping of these data showed that the

magnitudes of many of the values were reasonable, but a number of them were too large to be accepted. The gross-features of the scalar fields of liquid-water appeared to be physically reasonable.

A continuity equation for liquid-water content was developed in an effort to compute point values of the vertical speed in a cloud. This equation has an advantage over the continuity equation employed by Runnels [1962] and Clark [1964]. In the previously-used version it was assumed that the condensation of water vapor immediately produced large rain drops (100μ and larger in diameter). An integral expression for droplet growth by coalescence was used in the present equation in place of the condensation term. The use of a term for growth of drops by coalescence is more appropriate for a radar study since drops are not detected until their diameters are approximately 100μ. To reach this size, growth is assumed to be by the coalescence mechanism. The coalescence term also makes it possible to account for the downward development of an echo at a speed that is faster than the fall speed of raindrops. This effect has been reported as being a typical one [Byers, 1965].

The point values of the vertical speeds computed from the continuity equation were vitiated by the compounding of the experimental errors. The scalar fields of w, for each echo, were quite unrealistic.

A study of the reduction of the errors of measurement indicated that reasonably accurate values of M ($\pm$ 16%) can be obtained

through the use of better experimental control of day-to-day variations and accurate instruments to measure the parameters affecting the measured quantities. The use of accurate test instruments would permit the reduction of the semi-objective estimates of the errors used in this study by ascertaining systematic corrections for a part of the error. The remaining random component will be much smaller.

This study also indicates that attempts to measure vertical speeds accurately by use of the continuity equation may be frustrated because of the compounding of the experimental errors. An analysis of the errors associated with the derivatives of the scalar field of M will have to be performed before a definite answer can be given to the question of the usefulness of the continuity equation as a measuring relation.

Reccommendations for Future Investigations

Before the accurate measurement of cloud parameters can be achieved, a careful study of the experimental design must be made. This study should consider the delineation of the errors involved and the establishment of experimental techniques which are conducive to greater efficiency and reliability.

Errors of measurement are conveniently divided into several types. A general division is one that separates errors into a systematic class and a random class. Systematic errors are the same for each observation with a given apparatus and usually

arise from errors of calibration, personal errors of a consistent nature, constant experimental conditions which are different from those for which the system was calibrated, imperfect technique, and/or inexact equations upon which the design of the apparatus is based. Random errors are the variations due to the working of a number of small yet uncontrolled variables. As the name suggests, these variations form a random sequence and they often arise from errors of judgment resulting from varying estimates, fluctuating conditions, and small disturbances of an electrical or mechanical nature.

The systematic errors may be determinate ones if they can be evaluated by some logical procedure. This procedure may be theoretical or experimental. A thorough investigation should be made in order to evaluate as many of the systematic errors as possible. When these errors are determinate, the error may be removed by application of a suitable correction. An additional effort should be made to list all possible sources of indeterminate systematic errors so these can be located or at least accounted for.

In order to locate the determinate systematic errors and their magnitudes, accurate test instruments should be used to measure the constants of the radar system such as the antenna gain, beam width, transmitted power, pulse length, and wavelength. Such measurements also will narrow the limits of the uncertainties of these quantities from the semi-objective estimates that are

currently available. After performing these measurements the compounded error of the experiment can be re-evaluated. The new value of the compound error should be checked against the variations of the power reflected from a steady target. If all the systematic errors are accounted for, the data obtained from the steady target should be distributed in a symmetrical manner with a single maximum and with a measure of dispersion comparable to the compounded error. Failure of these two to agree may indicate the presence of systematic errors that have not been accounted for.

It seems that accurate measurements of received power can be made only after the introduction of a technique that will permit accuracies of $\pm$ 0.5 dbm on a logarithmic scale. Perhaps a pulse integrator will be required.

After the accuracy of the system is improved and after the magnitude of the errors is determined, studies should be commenced in order to determine the systematic errors inherent in the equations which approximate the actual situation. Thereby the relationship between received power and rainfall may be put on a firmer basis than afforded by the present empirical relations.

REFERENCES

Ackerman, B., "The variability of the water contents of tropical cumuli," Journal of Meteorology, 16(2): 191-198, April, 1959.

Aden, A. L., "Back-scattering of electromagnetic waves from spheres and spherical shells," Geophysical Research Paper No. 15, Geophysics Research Division, Air Force Cambridge Research Center, Cambridge, Massachusetts, July, 1952.

Anderson, C. E., "A study of the pulsating growth of cumulus clouds," Geophysical Research Paper No. 72, Geophysics Research Division, Air Force Cambridge Research Laboratories, Bedford, Massachusetts, 1960.

Atlas, D., "The estimation of cloud parameters by radar," Journal of Meteorology, 11(4): 309-317, August, 1954.

_____, "Advances in radar meteorology," Advances in Geophysics, Vol. 10, Academic Press, New York, pp. 318-483, 1964.

_____, and Banks, H. C., "The interpretation of microwave reflections from rainfall," Journal of Meteorology, 8(5): 271-282, October, 1951.

_____, and Mossop, S. C., "Calibration of a weather radar using a standard target," Technical (Scientific) Note No. 1, Contract No. AF 61 (052)-254, Imperial College of Science and Technology, London, Department of Meteorology, September, 1959.

Austin, P. M., and Geotis, S., "The radar equation parameters," Proceedings of the Eighth Weather Radar Conference, American Meteorological Society, Boston, pp. 15-22, 1960.

Battan, L. J., "Observations on the formation and spread of precipitation in convective clouds," Journal of Meteorology, 10(5): 311-324, October, 1953.

_____, Radar Meteorology, University of Chicago Press, Chicago, 161 pp., 1959.

Beers, Y., Introduction to the Theory of Error, Addison-Wesley, Reading, Massachusetts, 66 pp., 1957.

Bent, A. E., Austin, P. M., and Stone, M. L., "Beam width and

pulse length in radar weather detection," Technical Report No. 12, Massachusetts Institute of Technology, Cambridge, 1950.

Blanchard, D. C., "Behavior of water drops at terminal velocity," Transactions of the American Geophysical Union, 31(6): 836-842, December, 1950.

Bowen, E. G., "The formation of rain by coalescence," Australian Journal of Scientific Research, Series A, 3(2): 193-213, June, 1950.

_____, "Radar observations of rain and their relations to mechanisms of rain formation," Journal of Atmospheric and Terrestrial Physics, 1(3): 125-140, May, 1951.

Braham, R. R., "The water and energy budgets of the thunderstorm and their relation to thunderstorm development," Journal of Meteorology, 9(4): 227-242, August, 1952.

Byers, H. R., Elements of Cloud Physics, University of Chicago Press, Chicago, 191 pp., 1965.

_____, and Braham, R. R., The Thunderstorm, United States Government Printing Office, Washington, 287 pp., 1949.

_____, and Hall, R. K., "A census of cumulus-cloud height versus precipitation in the vicinity of Puerto Rico, Winter-Spring, 1953-1954," Journal of Meteorology, 12(2): 176-178, April, 1955.

Clark, R. A., "A study of convective precipitation as revealed by radar observation, Texas 1958-59," Journal of Meteorology, 17(4): 415-425, August, 1960.

_____, "The feasibility of a dual-frequency radar system in studying the morphology of subtropical precipitation," Ph.D. Dissertation, Department of Oceanography and Meteorology, Texas A&M University, College Station, Texas, 1964.

Donaldson, R. J., "Methods for identifying severe thunderstorms: a guide and bibliography," Bulletin of the American Meteorological Society, 46(4): 174-193, April, 1965.

Fanning, R. W., "An investigation of the applicability of analytically manageable raindrop size distributions to radar observations of subtropical precipitation," M. S. Thesis, Department of Oceanography and Meteorology, Texas A&M University, College Station, Texas, 1965.

Fletcher, N. N., The Physics of Rainclouds, Cambridge University Press, Cambridge, England, 386 pp., 1962.

Greene, D. R., "An investigation of precipitation attenuation and its application in a dual-frequency radar morphology of subtropical precipitation," M. S. Thesis, Department of Oceanography and Meteorology, Texas A&M University, College Station, Texas, 1964.

Griffiths, J. F., private communication, 1967.

Hitschfeld, W., and Bordan, J., "Errors inherent in the radar measurement of rainfall at attenuating wavelengths," Journal of Meteorology, 11(1): 58-67, February, 1954.

Houghton, H. G., "On the physics of clouds and precipitation," Compendium of Meteorology, American Meteorological Society, Boston, pp. 165-191, 1951.

Howell, W. E., "The growth of cloud in uniformly cooled air," Journal of Meteorology, 6(2): 134-149, April, 1949.

Huebner, G. L., Jr., private communication, 1967.

Johnson, J. C., Physical Meteorology, John Wiley & Sons, Inc., New York, 393 pp., 1954.

Kerr, D. E., (editor), Propagation of Short Radio Waves, Vol. 13, M. I. T. Radiation Laboratory Series, McGraw-Hill, New York, 728 pp., 1951.

Kessler, E., "Kinematical relations between wind and precipitation distributions," Journal of Meteorology, 16(6): 630-637, December, 1959.

_____, "Kinematical relations between wind and precipitation distributions, II," Journal of Meteorology, 18(4): 510-525, August, 1961.

_____, "Relationships between tropical precipitation and kinematic cloud models," Report No. 3 from Travelers Research Center to the Department of the Army on Contract DA 36-039 SC 89099, 1963.

Langmuir, I., "The production of rain by a chain reaction in convective clouds at temperatures above freezing," Journal of Meteorology, 5(5): 175-192, October, 1948.

Ludlam, F. H., "The physics of ice clouds and mixed clouds,"

Compendium of Meteorology, American Meteorological Society, Boston, pp. 192-198, 1951.

Marshall, J. S., and Palmer, W. McK., "The distribution of raindrops with size," Journal of Meteorology, 5(4): 165-166, August, 1948.

Mason, B. J., The Physics of Clouds, Oxford University Press, London, 481 pp., 1957.

_____, and Chien, C. W., "Cloud drop growth by condensation in cumulus," Quarterly Journal of the Royal Meteorological Society, 88(376): 136-142, April, 1962.

Mie, G., "Beiträge zur optick trüber medien, speziell kolloidaler metallösungen," Annalen der Physik, 25(3): 377-445, March, 1908.

Mordy, W., "Computations of the growth by condensation of a population of cloud droplets," Tellus, 11(1): 16-44, February, 1959.

Moyer, V. E., "Radar modification," Final Report on Grant NSF GP-2871, Department of Oceanography and Meteorology, Texas A&M University, College Station, Texas, May, 1965.

Mueller, E. A., "Raindrop distributions at Miami, Florida," Illinois State Water Survey Research Report No. 9B, June, 1962.

Probert-Jones, J. R., "The radar equation in meteorology," Quarterly Journal of the Royal Meteorological Society, 88(378): 485-495, October, 1962.

Reid, R. O., private communication, 1967.

Rigby, E. C., Marshall, J. S., and Hitschfeld, W., "The development of the size distribution of raindrops during their fall," Journal of Meteorology, 11(5): 363-372, October, 1954.

Runnels, R. C., "Kinematical relations among radar-observed water concentration, vertical motions, and liquid-water drop-size distributions in convective clouds," M. S. Thesis, Department of Oceanography and Meteorology, Texas A&M University, College Station, Texas, August, 1962.

Semonin, R. G., "Experimental and theoretical investigation of the coalescence of liquid drops," Illinois State Water

Survey Final Report under National Science Foundation Grant GP-2528, February, 1967.

Squires, P., "The micro-structure of cumuli in maritime and continental air," Tellus, 8(4): 443-444, November, 1956.

Stephens, J. J., "Radar characteristics of an exponential drop-size distribution with application to a dual-frequency system," National Science Foundation Grant NSF G-22115, Electrical Engineering Research Laboratory, The University of Texas, Austin, October, 1962.

_____, "On the applicability of Rayleigh scattering in radar meteorology," Journal of Applied Meteorology, 3(2): 211-212, April, 1964.

Telford, J. W., "A new aspect of the coalescence theory," Journal of Meteorology, 12(5): 436-444, October, 1955.

Von, V. M. H., "Theoretical investigation of the applicability of a dual-frequency radar system to the study of convective liquid precipitation," M. S. Thesis, Department of Oceanography and Meteorology, Texas A&M University, College Station, Texas, May, 1963.

_____, Clark, R. A., Stephens, J. J., and Moyer, V. E., "An investigation of Mie and Rayleigh backscattering at 3.2- and 10.3-centimeter wavelengths," Journal of Geophysical Research, 69(14): 2873-2880, July 15, 1964.

Wexler, R., "Rain intensities by radar," Journal of Meteorology, 5(4): 171-173, August, 1948.

Wilson, E. B., Jr., An Introduction to Scientific Research, McGraw-Hill, New York, 375 pp., 1952.